Chitin Metabolism by *Vibrio furnissii*: Quantification of *nagE* Expression

by
Sarah G. Brown

A Thesis Submitted in Partial Fulfillment

of the Requirements for the Degree

Master of Science

Major Subject: Interdisciplinary Sciences

West Texas A&M University

Canyon, Texas

May 2017

Abstract

The phosphoenolpyruvate: sugar phosphotransferase system (PTS) was first discovered in the 1960s by Kundig et al. The PTS is unique to bacteria, and is a rich area of study offering an abundance of potential research topics due to its environmental role and its potential as a target for future antibiotics. This study focuses on the *nag* operon, which plays an important role in chitin degradation. The expression of *nagE*, one gene located on the *nag* operon, was assessed via quantitative PCR (qPCR) in the presence of four substrates. This gene encodes the *N*-acetylglucosamine transporter protein. Expression of the gene was found to be up-regulated in the presence of *N*-acetylglucosamine, but not in the presence of glucose, mannose, or lactate. Potential future projects include: the quantification of expression of *nagA* via qPCR; the use of a reporter gene to quantify expression of *nagE* and *nagA*; study of NagC, thought to be the repressor of the *nag* operon; and further study and characterization of the gene encoding for the glucose specific transporter protein in *V. furnissii*.

Acknowledgements

I would like to thank Dr. Carolyn Bouma, first and foremost, for her invaluable guidance and expertise, as well as her time, patience, and encouragement during the course of this project. I would also like to thank Dr. Donna Byers, for time spent instructing me on how to carry out a gene expression study using qPCR, as well as the use of her Nanodrop system; Dr. Stephen Karaganis for the use of his real-time thermal cycler system; Dr. Rocky Ward, for use of his thermal cycler and sequencer; Dr. James Stoll at the Texas Tech University Health Science Center School of Pharmacy, for use of the Nanodrop spectrophotometer to determine DNA concentration; and Dr. David Khan for the use of his spectrofluorometer. I am grateful to Dr. Nick Flynn, Dr. David Sissom, Dr. Douglas Bingham, Dr. Gene Carlisle, Dr. Shiquan Tao, and Dr. Richard Kazmaier for guidance and support. I am also grateful to Alyssa Lemos, for her collaboration on working out the protocol for the CAT Assay, Juliana Morias for her assistance in measuring bacterial growth curves, and to Joshua Evans, for his preliminary work characterizing the strength of the *nagE* promoter. Finally, I would like to thank my mother, Esther Brown, and my grandmother, Evelyn Ariola for their support and patience throughout the duration of my academic career thus far.

Approved:

_____ _____
Chairperson, Thesis Committee Date

_____ _____
Member, Thesis Committee Date

_____ _____
Member, Thesis Committee Date

_____ _____
Member, Thesis Committee Date

_____ _____
Head, Major Department Date

_____ _____
Dean, Academic College Date

_____ _____
Dean, Graduate School Date

TABLE OF CONTENTS

Chapter **Page**

II. MATERIALS AND METHODS

List of Abbreviations

ATP – adenosine triphosphate

cAMP – cyclic adenosine monophosphate

Crp – cAMP receptor protein

Glc – glucose

GlcNAc – *N*-acetylglucosamine

Man - mannose

MIQE – Minimum Information for publication of Quantitative real-time PCR Experiments

ORF – open reading frame

PCR – polymerase chain reaction

PEP – phosphoenolpyruvate

PTS – phosphoenolpyruvate: sugar phosphotransferase system

qPCR – quantitative PCR

ROK – repressors, ORFs, kinases

RT – reverse transcription

List of Tables

Table **Page**

List of Figures

Figure **Page**

CHAPTER 1

INTRODUCTION

1.1 Bacteria and Geochemical Cycles

Microbial biochemical processes are intimately and inextricably linked with the environmental cycling of elements crucial to life as we know it, such as phosphorous, nitrogen, and, perhaps most importantly, carbon (5). The Global Carbon Cycle refers to an assortment of processes through which carbon is transformed from atmospheric CO_2 to organic matter by photosynthesis [and, to a lesser extent, carbon fixation by autotrophic microbes (7-13)] then subsequently transferred to the soil and sundry sediments. From soils and sediments, organic carbon is transported to the oceans by rivers, streams, and other runoff, where is it is eventually subducted as part of the ocean floor down into the Earth's interior. Finally, volcanic and other geothermic activity emit CO_2 back into the atmosphere again (22).

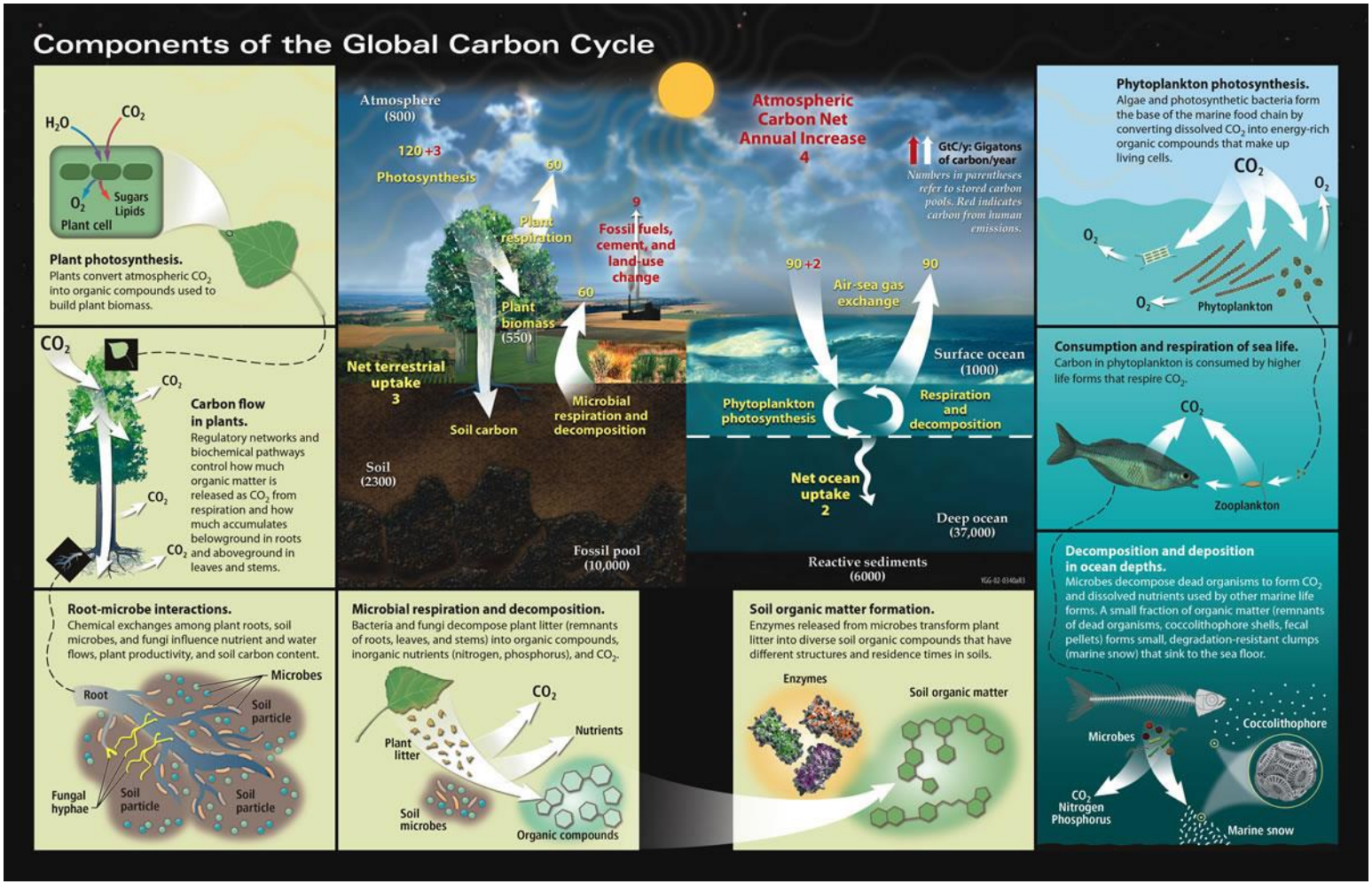

Figure 1. Components of the Global Carbon Cycle

Volcanic activity not depicted in this figure. Numerical data represents gigatons of carbon exchanged.
Image: source: U.S. Department of Energy (2). Used with permission.

As the first forms of life on Earth, bacteria have had millions of years to integrate themselves into Earth's elemental cycles that are essential to present-day life. In fact, the appearance of O_2 in the Earth's atmosphere, critical to the process of cellular respiration (1), can be attributed to the metabolic processes of prokaryotic organisms (22). Although they are not the only organisms participating in the cycling of essential minerals, some crucial environmental processes are carried out exclusively by specific bacterial species (5).

Despite the many processes involved in the cycling of essential elements, however, the Earth's biosphere does not typically function in a state of precise chemical equilibrium (5). The disequilibrium of the biosphere is a result of the influence of human activity as well as limitations placed upon rates of reactions by factors such as physical proximity of reactants, reaction kinetics, chemical transport demands, and specialized substrate requirements of different decomposer species (5, 22, 24). When studying the cycles of elements on a global scale, scientists sometimes compartmentalize habitats and their organisms into systems which serve as "reservoirs" for particular elements (24). A relative steady state must be maintained between an organism and its environment on the level of the organism. To maintain a steady state, an organism must draw on the resources of one of the nearby reservoirs of essential elements in some form or fashion.

Eukaryotic cells enjoy the benefit of subcellular environmental control via the biochemical processes of the organism. In contrast, unicellular prokaryotes must be able to adapt to extreme and sudden changes in their environment. Centuries of adaptation has led to the development of complex metabolic pathways which are able to effectively

utilize nearby available nutrients in exchange for the least amount of energy expenditure possible. The study of the carbon cycle on the macroscopic and microscopic levels has become increasingly important since the industrialization of human civilization, which has led to an extreme increase in CO_2 emissions into the atmosphere and the seemingly inevitable prospect of global warming.

It is important to understand the role that bacteria play in the crucial cycling of essential elements. To understand this, we must first determine how bacterial metabolic processes are carried out within the cell. Intracellular transport is the first step towards metabolism, and bacteria accomplish transport by a variety of means. Passive pathways include diffusion, facilitated diffusion, and osmosis, while active pathways include active transport and group translocation (25). In all forms of passive transport, substrates flow from regions of higher concentration to regions of lower concentration; no energy is expended to obtain nutrients via passive transport. Active transport and group translocation, however, take place against the concentration gradient of the substrate, and therefore must be coupled to exergonic reactions, like the transfer of a phosphoryl group from a high-energy compound such as adenosine triphosphate (ATP) or phosphoenolpyruvate (PEP) (1).

Bacteria can be classified as either Gram-positive or Gram-negative depending on the composition of their cell walls (25). These two types of bacteria were originally distinguished by the Gram staining technique, developed by Hans Christian Gram in 1884 (25, 26). Both Gram-positive and Gram-negative bacteria utilize a rigid peptidoglycan layer, composed of β-linked *N*-acetylglucosamine and *N*-acetylmuramic

acid, to serve as a supporting structure, since prokaryotes lack a cytoskeleton (5, 25) and both have a cytoplasmic membrane which is comprised of a phospholipid bilayer and associated proteins. However, Gram-positive bacteria have a much thicker peptidoglycan layer. Furthermore both Gram-negative and Gram-positive bacteria also possess a second bilayer membrane, and the peptidoglycan layer exists between the inner and outer membrane as shown in **Figure 2** (next page). In Gram-negative bacteria, the outer bilayer membrane consists of an inner leaflet of phospholipids, and an outer leaflet of lipopolysaccharides as well as integral, peripheral, and glycoproteins (25). The region between the inner and outer membranes is referred to as the periplasmic space, and is relatively large in Gram-negative bacteria. A much smaller periplasmic space has recently been observed and reported in some Gram-positive bacteria (27-29).

Prokaryotes exist in diverse shapes, the most common of which are cocci (spherical) and bacilli (rod-shaped). *Escherichia coli* is a Gram-negative bacillus that is commonly used to study bacterial systems. *Vibrio furnissii*, the organism of interest in this study, is a Gram-negative curved-rod (30). Refer to **Figure 3** (page 7) for the general structure of a rod-shaped prokaryote.

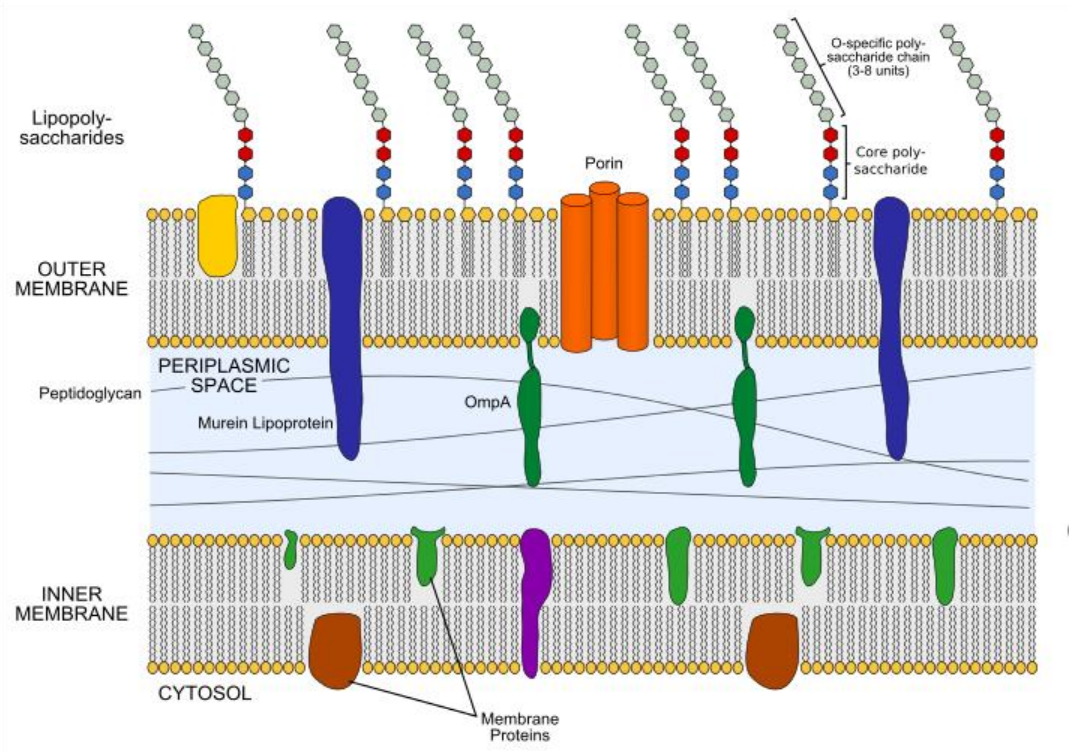

Figure 2. The periplasmic space of a Gram-negative bacterium. The peptidoglycan layer is located between two phospholipid bilayers. Chitin and other saccharides may be transported into the periplasmic space as disaccharides, oligosaccharides, or monosaccharides via specific porins that span the outer phospholipid bilayer. Substrate specific transporter proteins belonging to the bacterial PTS span the inner phospholipid bilayer. Image source: © Jeff Dahl (6). Creative Commons.

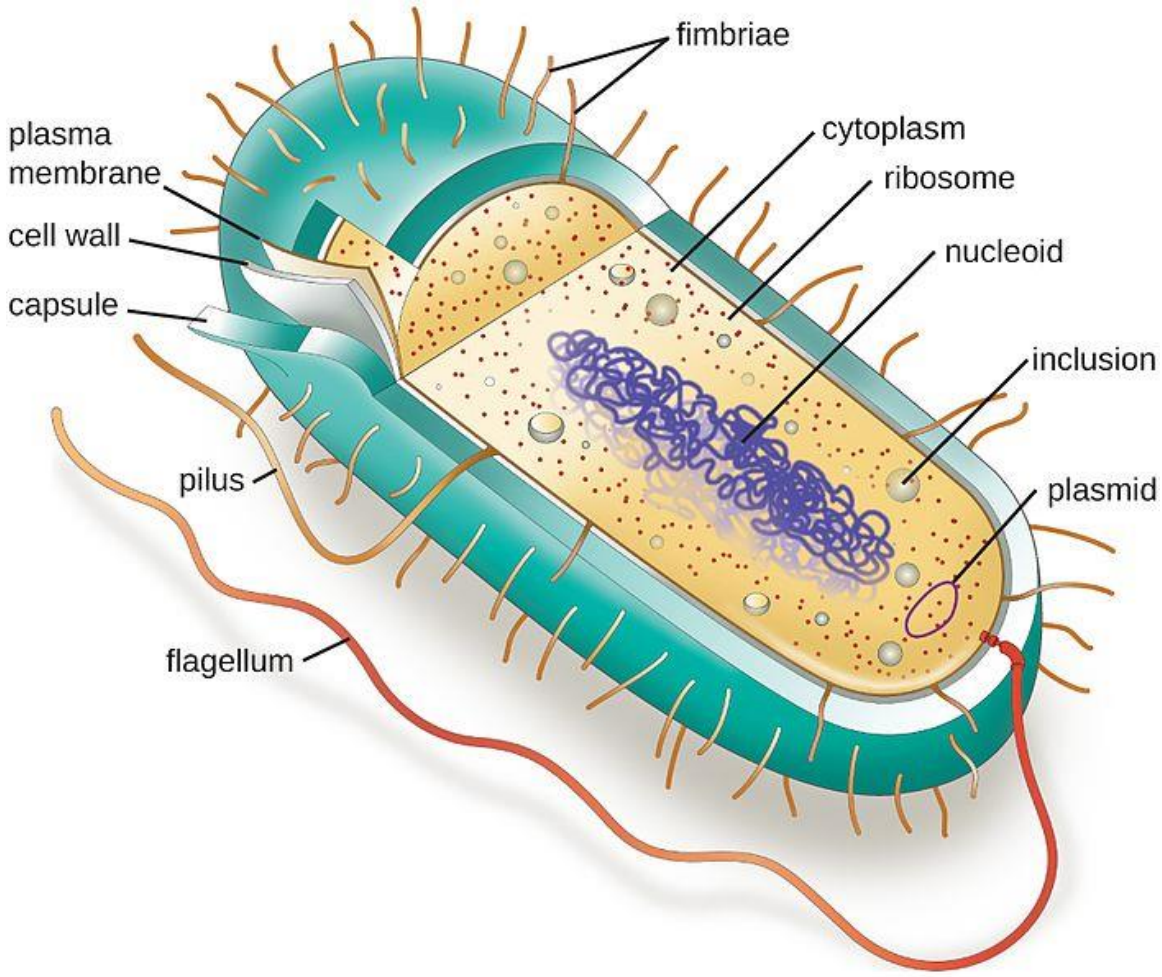

Figure 3. A typical rod-shaped prokaryote, similar to *Escherichia coli*.
V. furnissii, a curved-rod bacterium, also possesses both polar and lateral flagella, functional for swimming in the aqueous environment of the ocean and across solid surfaces, respectively. Image source: *Microbiology*, v. 4.4 (Online) (3). Creative Commons.

Of course, in addition to being helpful organisms which participate in various environmental cycles essential to life, bacteria can also be detrimental to the health of eukaryotic organisms, causing sickness and even death. By exploring metabolic pathways of bacteria, we enhance not only our collective knowledge of the diverse ways that bacteria participate in the cycling of essential elements, but we may also increase our valuable arsenal of antibiotics and bacteriostats used to combat infections and diseases caused by bacteria. Antibiotic resistance in infectious bacteria is becoming an increasingly alarming and important problem which will require ingenuity to solve (31-34). Any information which could lead to the development of new antibiotics is crucial.

However, the metabolic pathways of bacteria are complex, and elucidating the specific molecular mechanisms often requires a series of experiments or projects. This dissertation focuses chiefly on the *nag* operon of *Vibrio furnissii* and its role in the carbon cycle involving the metabolism of *N*-acetylglucosamine, the monomer of chitin. The *nag* operon is just one small part of a complex metabolic system known as the phosphoenolpyruvate: carbohydrate phosphotransferase system (PTS) in this marine dwelling bacterium.

1.2 Chitin, the second most abundant biopolymer on earth

Chitin (**Figure 4a**, page 11), the second most abundant biopolymer on Earth, is outranked in abundance by only cellulose (35). This polysaccharide is found in the Kingdoms Fungi, Plantae, and most abundantly in Animalia. Within the Kingdoms Fungi and Plantae, chitin serves as an important structural component of the cell walls of mushrooms and molds, and some species of green algae (36-38). Within the Kingdom Animalia, chitin comprises the exoskeletons of insects (**Figure 4b**) and crustaceans (**Figure 4c**).

One reason for the prevalence of chitin may be its unique structural chemistry depicted in **Figure 4a**. *N*-acetyl-D-glucosamine (also commonly referred to as *N*-acetylglucosamine, GlcNAc, or NAG), the monomer of chitin, is an amino monosaccharide, meaning that it is a complex sugar with an amine group replacing one of the standard hydroxyl groups, and requires deamination and deacetylation before entering glycolysis. In GlcNAc, the hydroxyl group on carbon number two of glucose is replaced by an amine group (see **Figure 4a**). The presence of this amine group contributes to the durability of chitin. Other common examples of amino monosaccharides include galactosamine, glucosamine, and sialic acid. It is also a β-linked polysaccharide, which is more difficult to metabolize than an α-linked polysaccharide. Some Eukaryota form symbiotic relationships with bacteria in order to aide in the digestibility of β-linked, structural polysaccharides.

In addition to comprising the exoskeletons of insects and crustaceans, *N*-acetylglucosamine is also utilized by bacteria along with *N*-acetylmuramic acid to construct peptidoglycan, which is responsible for the durability of bacterial cell walls. GlcNAc is also found in the lipopolysaccharides present in the outer leaflet of the outer bilayer membrane in Gram-negative bacteria (25). GlcNAc is also used to a much lesser extent in humans, particularly in the glycosaminoglycan hyaluronan, which is an important component of the synovial fluid of the joints and the vitreous fluid of the eye, where it serves as a lubricant and shock absorber (1).

a.)

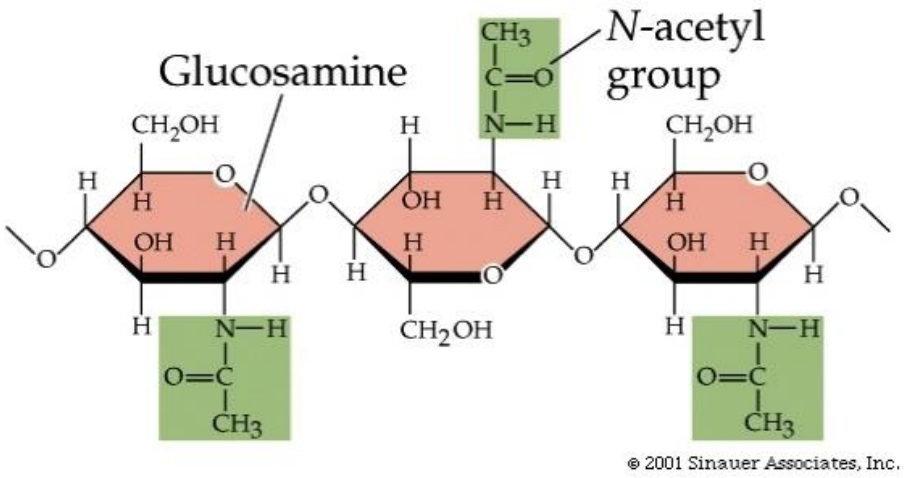

b.)

c.)

Figure 4. Chitin and examples of environmental sources of chitin

a.) Note the β-linkage between the monomers of GlcNAc, which each contain an amine group on carbon 2. Image source: *Life, the science of biology* 6th ed, Purves (4). Used with permission.

b.) Cicada shell, *Lyristes plebejus*. Image source: © Jodelet/Lépinay (18). Creative Commons.

c.) Crab shell, *Cancer pagurus*. Image source: © Hans Hillewaert (21). Creative Commons.

Chitin is particularly abundant in the marine environment. Debris from the exoskeletons of zooplankton alone produce well over billions of tons of chitin annually (39) (see **Figure 5**, p 13). Chitin is converted from a sequestered form to biologically usable forms of carbon and nitrogen at a truly prodigious rate. Only a small amount of carbon (2 gigatons) sinks to the ocean floor annually; the majority of fixed carbon (90 gigatons) is decomposed and transformed back into biologically usable forms (refer to **Figure 1**) (2). Naturally, chitinolytic bacteria were found to be responsible for such a immense process (40).

Vibrio furnissii is a chitinolytic strain of bacteria that lives in the ocean. It was discovered in 1983 by Brenner and company when it was isolated from both human feces and the environment (41) and was shown to adhere more avidly to GlcNAc beads than 7 other chitinolytic *Vibrio* strains tested in 1991 (42). The bacterial family Vibrionaceae is closely related to the more well studied family of Enterobacteriaceae which includes the species *Escherichia coli*, a species that is more extensively studied and understood than *V. furnissii* (43). It is worth noting that *E. coli* does not degrade chitin, although it does contain a *nag* operon (see **The *nag* and *man* operons** on page 28 for more details).

In *V. furnissii* and in other species of *Vibrio*, GlcNAc is processed as a source of carbon and energy by the bacterial phosphotransferase system (42). Trehalose (found in the hemolymph of insects and crustaceans), GlcNAc, and glucose (Glc) have been shown to be potent chemoattractants of *V. furnissii* (16).

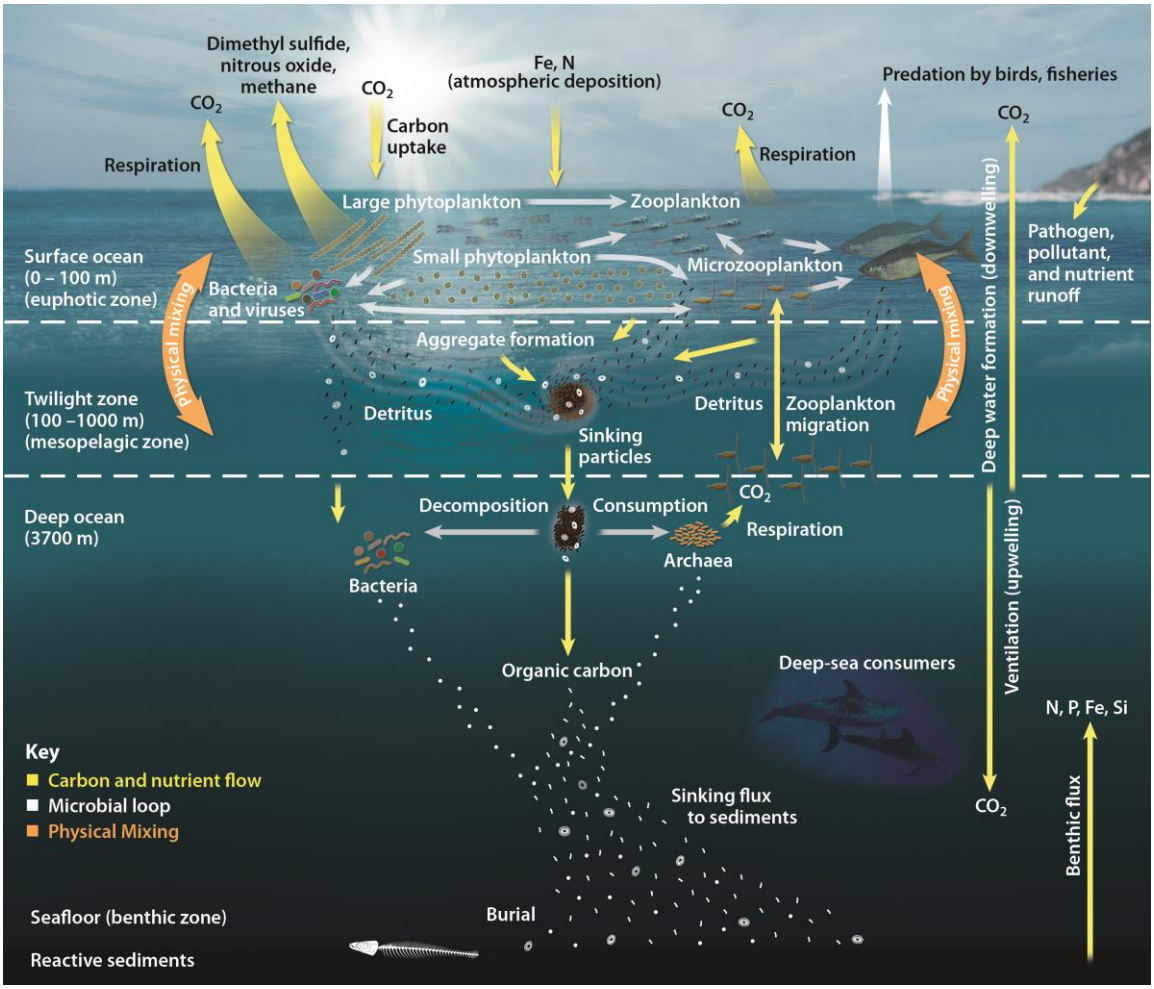

Figure 5. Carbon flow and fate in the marine ecosystem. Chitin is an important source of carbon and nitrogen within marine ecosystems. Autotrophic phytoplankton sequester CO_2 in the form of glycogen and chitin and are grazed upon by larger organism. The exoskeletons of these phytoplankton (and larger crustaceans) are in turn decomposed into biologically useful forms of carbon and nitrogen by heterotrophic, chitinolytic bacteria. Image source: U.S. Department of Energy (2). Used with permission.

1.3 Metabolism of chitin

Chitinolytic bacteria sense and swim toward chitin sources in a process known as chemotaxis. As a result, bacterial populations are two to five times higher near a chitin source as compared to normal sea water. When *V. furnissii* senses a gradient of GlcNAc, extracellular hydrolytic enzymes (chitinases) are secreted (16). These chitinases hydrolyze the chitin polymer into smaller fragments, increasing the chemotactic gradient, as shown in **Figure 6** (next page).

$GlcNAc_n$ oligomers (n = 2-6) are transported into the periplasmic space (see **Figure 2**, page 6) of *V. furnissii*, most likely via a specific chitinoporin, Chi P (44). Within the periplasmic space, the chitin oligomers undergo further degradation by chitinodestrinase, which cleaves soluble chitin oligomers (45), and β-*N*-acetylglucosaminidase, which hydrolyzes GlcNAc from the terminal end of chitin oligomers (46). The integral membrane protein NagE is responsible for transporting the monomer GlcNAc from the periplasmic space into the cytoplasm. This permease phosphorylates GlcNAc as it is transported into the cell, where it is subsequently deactylated and deaminated in preparation for further catabolism (47). Interestingly, *V. furnissii* is also thought to transport *N,N'*-diacetylchiobiose, $(GlcNAc)_2$, into the cytoplasm via a specific disaccharide transport system (48). However, this transport protein remains to be isolated.

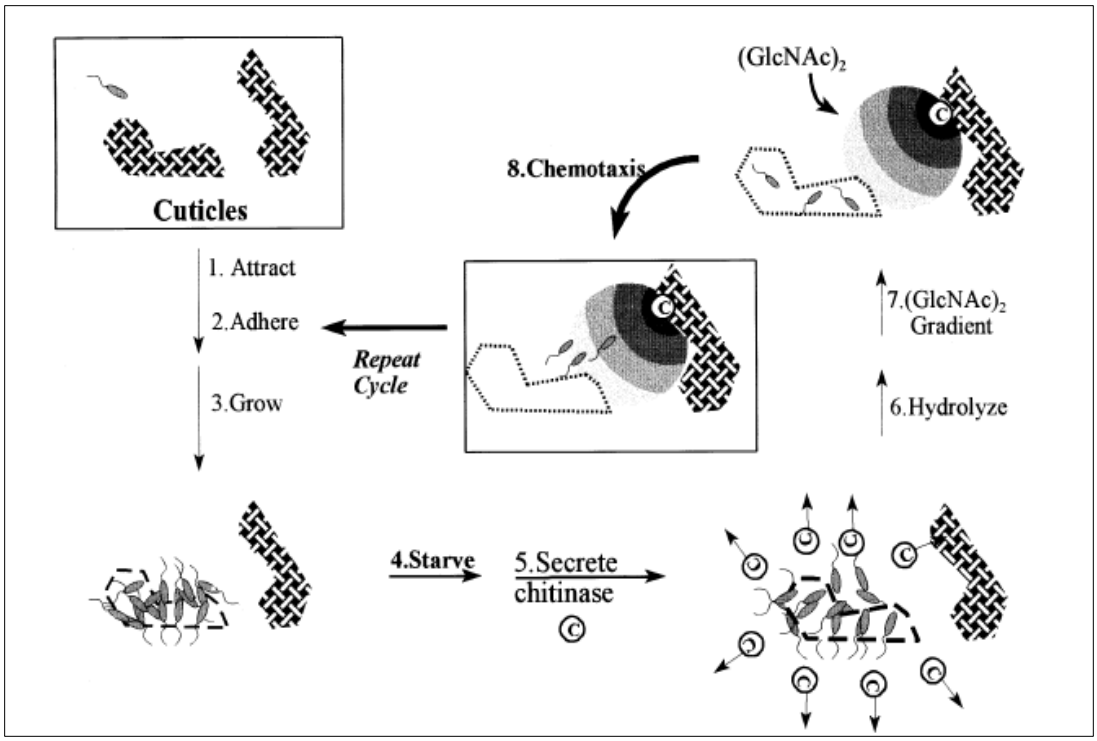

Figure 6. The "chitin catabolic cascade." C represents the hydrolytic enzyme, chitinase. Chitinase is secreted when *V. furnissii* senses a chitin source. As the chitin is hydrolyzed, the chemotactic gradient is increased, attracting nearby bacteria to the source. Image source: *Physiological aspects of chitin catabolism in marine bacteria*, Keyhani and Roseman (16)**.** Used with permission.

1.4 The environmental and clinical role of *Vibrios*

The genus *Vibrio* contains over 30 species and includes at least 12 species which are associated with human disease (typically intestinal) (49). *Vibrio* are widely distributed in aquatic environments throughout the world (49), and presumably play a significant role in the aquatic ecosystem due their role in degrading chitin (42). Among disease-causing species of *Vibrio*, *V. cholerae* is perhaps the most well-known. The first documented cholera outbreaks took place in the late 1700s in Calcutta, India (50). Since then, the disease has caused several severe epidemics throughout the world. Cholera remains a problem in poorer countries with inadequate water sanitation systems and limited access to medical supplies (51). Other known causative agents of disease belonging to the genus *Vibrio,* which can cause vibriosis presenting as a form of gastroenteritis or septicemia, include but are not limited to *V. parahaemolyticus*, *V.vulnificus*, *V. alginolyticus*, *V. damsela*, *V. fluvialis*, *V. furnissii*, *V. hollisae*, *V. metschnikovii*, and *V. mimicus* (49). Several species of *Vibrio* have been shown to be chitinolytic, among them *V.cholerae* (52), *V. furnissii* (42) and *V. harveyi* (13). Although *Vibrio* is an important genus both clinically and environmentally (particularly in the carbon cycle of aquatic ecosystems), many of its biochemical and metabolic functions are not well characterized.

1.5 The species *Vibrio furnissii*

Vibrio furnissii, originally thought to be an aerogenic subspecies of *V. fluvialis*, was first recognized as a separate species in 1983 (41). Its pathogenic potential was most recently evaluated in 2014 by Lux, Lee, and Love (53). According to this study, *V. furnissii* lacks the major pathogenicity islands found in the genome of its more toxic cousin, *V. cholerae*. However, natural competency and a high frequency of horizontal gene transfer raises suspicions that it may be an emerging pathogen, particularly to marine arthropods. According to the International Encyclopedia of Public Health, there have been zero deaths reported that were directly related to *V. furnissii* (54), although there have been scattered cases of gastroenteritis (54, 55) and one case of wound infection (56). The American Biological Safety Association classifies *V. furnissii* as a low risk-organism, and no safety precautions beyond standard aseptic techniques are required for laboratory study of the organism in the United States (57).

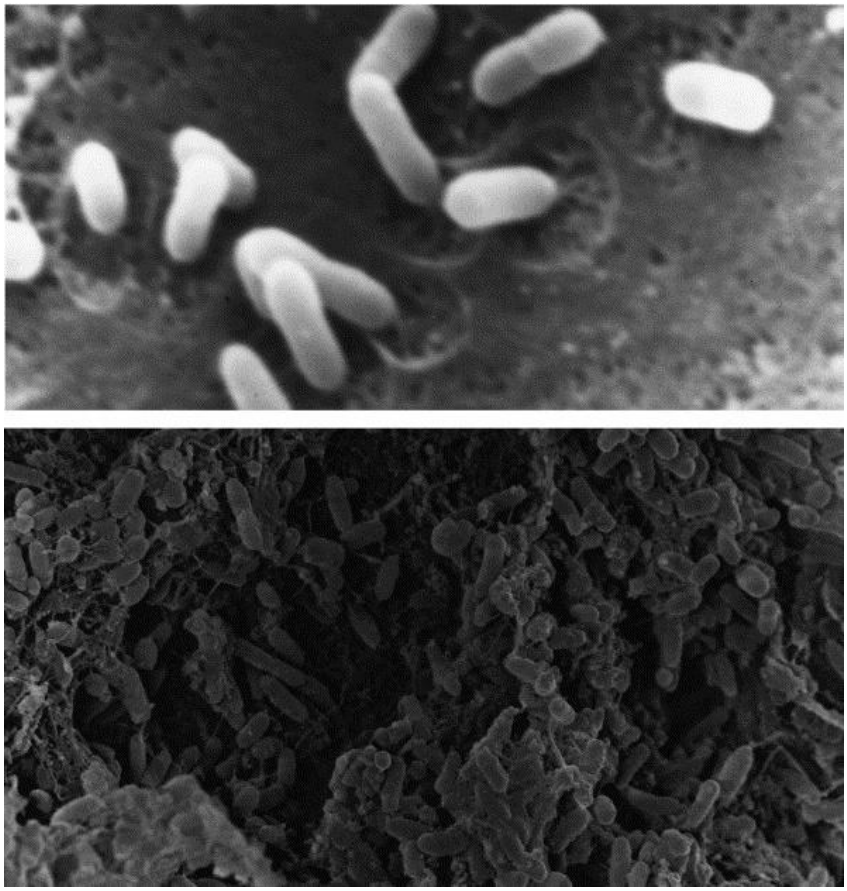

Figure 7. *Vibrio furnissii* degrading a chitin source. These photos show *V. furnissii* adhering to and degrading sources of chitin. Areas resembling pits or craters in the top image show where the chitin source has been digested. The bottom image shows bacteria associated with a marine snow aggregate. Image source: *Physiological aspects of chitin catabolism in marine bacteria*, Keyhani and Roseman (16)**.** Used with permission.

.

1.6 The phosphoenolpyruvate: carbohydrate phosphotransferase system in bacteria

The bacterial phosphoenolpyruvate: carbohydrate phosphotransferase system (PTS), employed for the transportation and metabolism of carbohydrates, was first isolated and characterized in cellular extracts of *Escherichia coli* by Kundig et al. roughly fifty years ago (58). Around this same time period, a pleiotropic mutant of *Staphylococcus aureus* unable to grow on a variety of carbohydrates was described by Egan and Morse (59-61). Murphey and Rosenblum described another mutant of *S. aureus* unable to grow on mannitol (62, 63). Indeed, such pleiotropic effects were described as early as 1949 (64). It was becoming apparent that the proteins of interest were components of a widely distributed bacterial transport and phosphorylation system (65).

Since its discovery, the PTS has been an area of intense research in many bacterial species (19, 43, 47, 65-80). Various forms of the PTS have been observed and studied in both enteric and non-enteric as well as both Gram-positive and Gram-negative bacteria (19, 68, 80). The common function of the PTS is chiefly the concomitant transport and phosphorylation of carbohydrates which are subsequently metabolized as sources of carbon and energy. The PTS has also been observed to take part in the regulation of non-PTS metabolic pathways, chemotaxis towards nutrients, biofilm formation, and virulence of infectious organisms (20, 75). The two main processes of regulation involve either down-regulation (usually in response to catabolite repression) or up-regulation (usually in response to inducing substrates) of certain genes and operons.

All phosphotransferase systems observed thus far have been found to consist of at least three enzymes, each of which can exist in both the phosphorylated and de-phosphorylated state: i) soluble enzyme I (EI), ii) soluble histidine phosphorylatable protein (HPr), and iii) an integral membrane protein, enzyme II (EII). EIIs are substrate specific to varying degrees and may be comprised of up to four different domains: i) EIIA, a small, hydrophilic subunit phosphorylated at a conserved His residue that is typically soluble and resides in the cytoplasm, but can also be bound to the other EII domains, ii) EIIB, another small, hydrophilic subunit that can either be soluble or bound to EIIC, which is phosphorylated at a conserved Cys residue, iii) EIIC, which is membrane-bound and spans the inner phospholipid bilayer, and iv) EIID which, when present, is bound to EIIC and also spans the inner phospholipid bilayer (75, 76). These enzymes are depicted in **Figure 8** (next page).

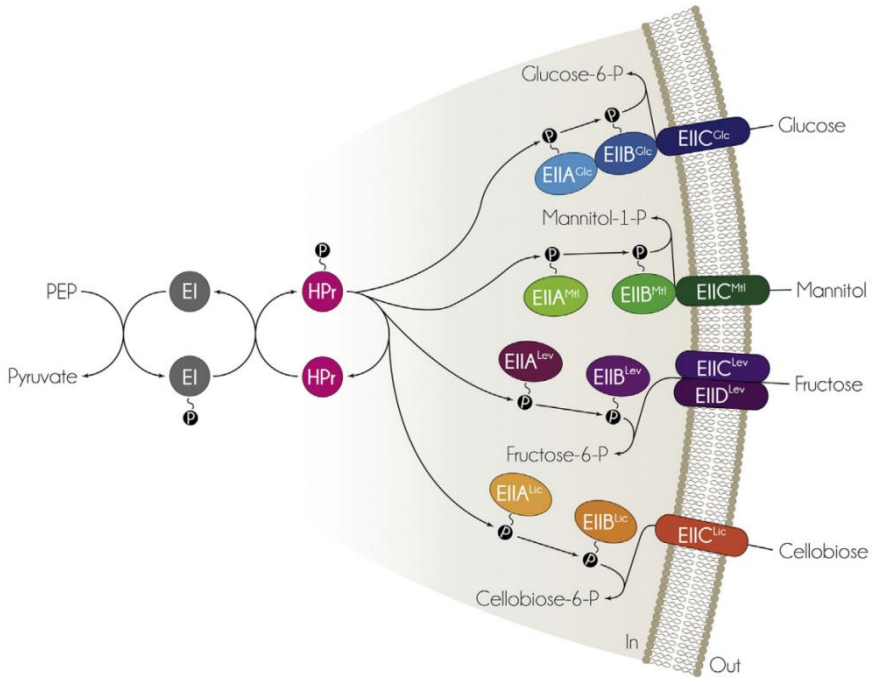

Figure 8. The Phosphoenolpyruvate: carbohydrate Phosphotransferase System. Carbohydrates taken up and phosphorylated by the PTS feed into glycolysis. The phosphorylation state of the PTS enzymes has been linked to the control of various prokaryotic systems, including the regulation of PTS and non-PTS catabolic enzymes, biofilm formation, and virulence in certain infectious organisms. This image depicts the structure of four phosphotransferase systems observed within the bacterium *Bacillus subtilis.* Image source: *Sophisticated Regulation of Transcriptional Factors by the Bacterial Phosphoenolpyruvate: Sugar Phosphotransferase System*, Galinier and Deutscher (20). Used with permission.

The bacterial PTS has recently undergone comparative genomic analyses across 202 genomes, including 173 bacterial species (80). Within the bacterial species analyzed, 57% were found to possess at least one complete PTS (including a substrate specific permease), 21% possess cytoplasmic PTS phosphoryl transfer proteins, but do not encode a membrane integrated permease, and 22% lack any recognizable PTS protein homologues. Permeases belonging to the glucose and fructose families were found to be the most prevalent. Nineteen species from the Domain Archaea and 10 species from the Domain Eukaryota were also analyzed and were found to lack PTS homologues. Only phosphoenolpyruvate synthases and pyruvate:phosphate dikinases are conserved across all three Domains. A single HPr kinase homologue has also been documented within one organism belonging to the Domain Archaea (81). The findings from this study support the theory that the PTS is unique to prokaryotes, likely evolving after the division of the Domains Bacteria, Archaea, and Eukaryota (82). It also seems likely that components of the PTS, particularly the integral membrane permeases, have been repeatedly gained and lost by various bacterial species due to mechanisms such as horizontal gene transfer (80, 83).

The structural genes of the PTS enzymes EI and HPr are located on the *pts* operon. EI and HPr are necessary for the phosphorylation of all EIIs, and are expressed constitutively. Furthermore, mutants deficient in EI and HPr are not only unable to process PTS substrates such as glucose, and mannose, but are also unable to grow on many non-PTS carbon sources, such as lactose, glycerol, maltose or melibiose (68, 75, 84).

EIIs are not located on the same operon as EI and HPr. They are instead each located on their own separate operons linked to the structural genes necessary for the metabolism of the EII specific substrate (75). The sugar substrate, or one of its metabolites, usually serves as the inducer for such an operon. Two such operons are the *nag*, and *man* operons of *Vibrio furnissii*, which are described further on page 28.

As described above, EIIs may consist of a single, membrane-bound protein or as a system of two to four protein domains at least one of which is membrane-bound. EIIs consisting of more than one protein (especially those involving a soluble EIIA protein) are sometimes involved in the regulation of PTS and non-PTS transport systems. For instance, $EIIA^{Glc}$ in *E. coli* is known to be involved in the regulation of the transport and/or metabolism of several PTS and non-PTS carbohydrates (68). The process by which $EIIA^{Glc}$ does this is described in the next section (see **Metabolism of glucose**, page 26).

As mentioned, EIIs are considered substrate-specific. However, EII specificity is broadly expressed (75). They often recognize a family of structurally-related substrates rather than one specific substrate. Seven permease families have been established based on phylogeny of EII complexes: (i) glucose, (ii) fructose, (iii) lactose, (56) galactitol, (v) glucitol, (vi) mannose, and (vii) L-ascorbate (80). An increased binding affinity is observed between the EII and its chief substrate. Consequently, specific EIIs are named for their chief substrates (75). For instance, EII^{Man} is the major transport system for mannose in *E. coli*, but this integral membrane protein also recognizes, transports, and phosphorylates glucose, 2-deoxyglucose, fructose, methyl-α-glucoside, and

N-acetylmannosamine, as well as GlcNAc and glucosamine (GlcN) (72, 74, 75), and EII^{Nag} is able to recognize, transport, and phosphorylate glucose, methyl-α-*N*-acetylglucosamine, iodo-*N*-acetylglucosamine, and streptozotocin (47, 75). This serves to maximize the ability of the bacteria to take up highly-preferred sugars in the near vicinity.

Substrates of the PTS are taken up preferentially over non-PTS substrates, a phenomenon originally described as diauxie by Jacques Monod in 1949 (see **Figure 9**, next page) (23). This phenomenon is characterized by biphasic growth in the presence of both a PTS and a non-PTS substrate. Among the PTS substrates, it has been demonstrated that glucose, fructose, and mannose are taken up by more than one membrane-bound enzymatic system (75).

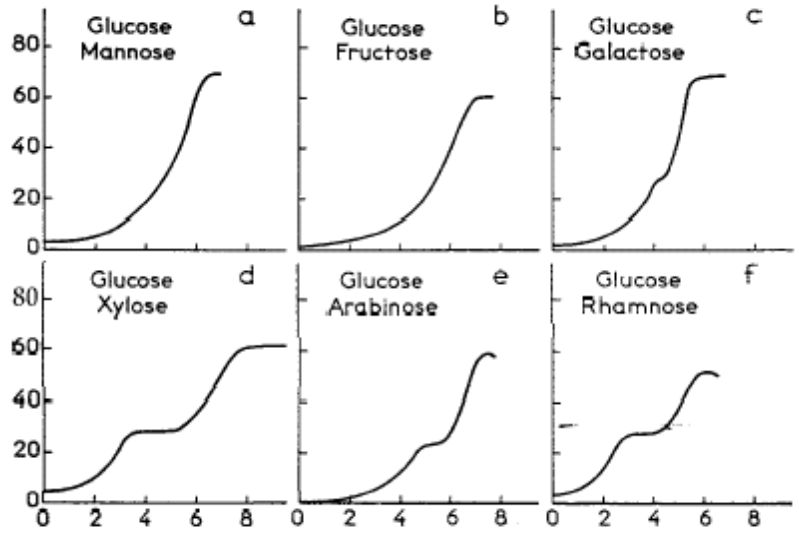

Figure 9. Diauxic growth as described by Jacques Monod. Diauxie describes a pattern of growth observed when a bacterial culture grown in two carbohydrate sources, with one carbohydrate source receiving preferential uptake. It is characterized by two phases of growth. Diauxie is not observed when glucose and fructose serve as the carbohydrate sources, however, due to an HPr-like domain found on the fructose-specific hybrid phosphotransferase protein, FPr, which can serve as a substitute for HPr in *E. coli* (19). Image source: *The growth of bacterial cultures*, Monod (23). Used with permission.

1.7 The metabolism of glucose

Because of its ability to be rapidly metabolized, glucose is taken up preferentially over all other PTS carbohydrates, resulting in a phenomenon known as the "glucose effect" (20, 68, 75). This effect is probably due to a decreased availability of the phosphorylated form of $EIIA^{Glc}$, since $P\sim EIIA^{Glc}$ is known to stimulate activity of adenylate cyclase and inhibit cyclic adenosine monophosphate (cAMP) phosphodiesterase (20, 68, 86). This leads to an increase in concentration of available cAMP (85). Synthesized cAMP then binds to the cAMP receptor protein (Crp). The Crp-cAMP complex is required in varying amounts by promoters[1] involved in the transcription of many peripheral enzymatic pathways, and is considered a global regulator in bacteria (20, 68).

When a bacterium is utilizing a nearby source of PTS substrate, such as GlcNAc or Glc, the phosphoryl group from $P\sim EIIA^{Glc}$ is required to phosphorylate the incoming substrate. The availability of $P\sim EIIA^{Glc}$ decreases, and thus the concentration of Crp-cAMP complex also decreases, which leads to a transient halt or slowing of the metabolic pathways required for processing non-PTS substrates. Recall that bacteria exhibit preferential uptake of PTS sugars over non-PTS sugars, a result of inducer exclusion characterized by diauxic growth (**Figure 9**, page 25). The regulation processes involved in the expression of this preference of PTS sugars over non-PTS sugars are not fully understood, but it has been speculated that phosphorylation state of other soluble PTS

1. Promoters are control sequences required for the binding of RNA polymerase and the initiation of transcription (1)

proteins may also play a regulatory role in peripheral carbohydrate transport systems in much the same way as $EIIA^{Glc}$ (19, 68, 80, 87) .

In *V. furnissii*, glucose is taken up by at least three PTS permeases and one non-PTS transport system (47, 67, 88). The DNA of isolated *ptsG* gene from *E. coli* was shown to hybridize to genomic DNA from *V. furnissii* (88). However, a glucose specific transporter equivalent to EII^{Glc} was not observed in the screening of 25,000 transformants (47). A *ptsG* homologue, presumably encoding the glucose specific permease, in *V. furnissii* has recently been sequenced (89), but exhaustive biochemical analysis has not yet been carried out.

1.8 The *nag* and *man* operons

Operons homologous to the *nag* and *man* operons have been identified in both Gram-positive and Gram-negative organisms (66, 78, 90), but the subject of this thesis is a Gram-negative organism, *V. furnissii*. Therefore only operons found within Gram-negative organisms will be discussed here.

The gene order for the *nag* operon in *E. coli* was first reported by Plumbridge in 1987 (73). By 1991, she had amended her findings to report the gene order *nagE-BACD* arranged on the operon with two divergently oriented promoters (74) (see **Figure 10a**, page 31), one initiating transcription of *nagE* and the other initiating the transcription of all other genes. The gene *nagE* is known to encode the EII^{Nag} transporter enzyme, also referred to as NagE in this thesis, while *nagB* and *nagA* encode GlcNAc-6-phosphate deaminase and GlcNAc-6-phosphate deacetylase, respectively, two enzymes which are necessary for the degradation of GlcNAc and GlcN (71). The metabolic pathway from periplasmic GlcNAc to intracellular Glc-6-P is shown below. The substrate Glc-6-P can feed into glycolysis.

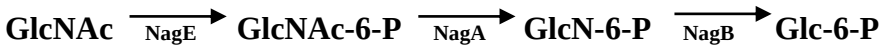

In *V. furnissii* the *nag* operon, *nagE-AC* (**Figure 10b**, page 31) is thought to encode the EII^{Nag} substrate specific transporter enzyme, GlcNAc-6-phosphate deacetylase, and the regulating protein NagC, in that order (47, 67). Like the *nag* operon in *E. coli*, transcription is thought to be under the influence of two divergently oriented promoters, with the transcription of *nagE* under control of one promoter and the transcription of *nagA* and *nagC* under control of the other.

The *man* operon in *E. coli* has also been studied, and the gene order was found to be *manXYZ*. The genes *manX*, *manY*, and *manZ* encode three separate proteins which together make up the EII^{Man} transport system (69, 70, 76). In addition to transporting and phosphorylating the sugar mannose, EII^{Man} also recognizes, phosphorylates, and transports glucose, 2-deoxyglucose, fructose, methyl α-glucoside, and *N*-acetylmannosamine, as well as GlcNAc and glucosamine (GlcN) (72, 74, 75) and is therefore considered a somewhat generic PTS-sugar transporter system, possibly used to scavenge for sugars derived from cell wall breakdown (19, 92). Mlc is the main repressor for this operon (92). In *V. furnissii*, the gene order is *manXYZW* and the EII^{Man} transporter protein is inactive with GlcNAc and fructose, although it does transport and phosphorylate glucose (67).

The product of *nagC* regulates the transcription of *nag* operon in the absence of GlcNAc (71). It does so by co-operative binding to two sites located near the divergently oriented promoter regions, causing the formation of a loop of DNA (93). In *E. coli*, when GlcNAc is available as a nutrient source, GlcNAc-6-P binds to NagC and causes the repressor to release the operator, allowing transcription of the genes located on the *nag*

operon (74). Interestingly, in the absence of GlcNAc, NagC has also been shown to activate the *glmUS* operon which encodes proteins necessary for the formation of UDP-GlcNAc (important for the synthesis of peptidoglycan) and the synthesis of GlcN (an important competent of bacterial lipopolysaccharides) (94). NagC is also known to bind to the *manX* locus of the *man* operon in *E. coli* (71), thus impeding the transcription of the entire operon. However, although the binding of NagC does inhibit transcription to a small extent, the binding of the protein Mlc has a much greater repressive effect on the *man* operon (74).

Mlc and NagC share ~40% identity with each other and are both members of the ROK (repressors, ORFs, kinases) family. Mlc is considered a global regulator of the PTS, and is known to bind to various operons, including the *mal* operon, the *man* operon, the *pts* operon (encoding the soluble PTS proteins EI, HPr, and $EIIA^{Glc}$), and the operator region for *ptsG* (72, 95). In the presence of dephosphorylated $EIICB^{Glc}$ (the main PTS transporter for glucose, also called PtsG), the repressor Mlc is sequestered to the membrane of the bacterium, which causes derepression of various genes, including genes which encode proteins related to the concomitant transport and phosphorylation of glucose (72, 95-97).

Both the *nag* and *man* operons have been shown to be dependent on the presence of the Crp-cAMP complex (92, 98), and both EII^{Man} and EII^{Nag} have been shown to transport and phosphorylate glucose in *V. furnissii* (47, 67). Glucose has also been shown to be taken up via a non-PTS transporter (88).

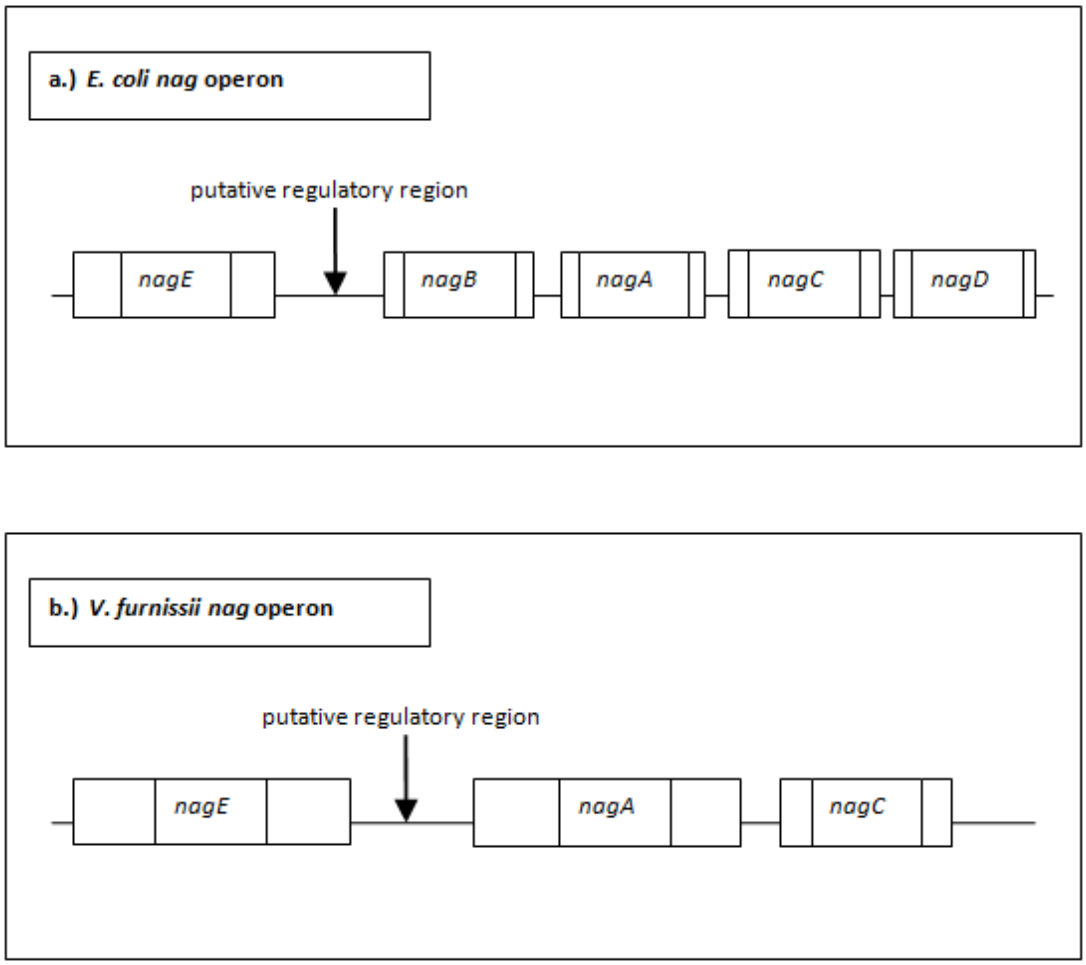

Figure 10. The *nag* operons of *E. coli* and *V. furnissii*

1.9 Conclusion

Understanding the roles that environmental bacteria play in major mineral cycles, such as the carbon cycle, may lead to better understanding and management of our biosphere, which is currently a matter of growing importance and concern. Additionally, understanding the transport systems by which bacteria locate and obtain nutrients may lead to novel antibiotics or bacteriostats. Our goal is to enhance the understanding of the specific mechanics of the phosphotransferase system in *V. furnissii*, an ecologically significant bacterial species. In this study, it is hypothesized that one or more sugars may regulate transcription of the *nag* operon due to substrate overlap and the complex nature of the bacterial PTS.

CHAPTER 2

MATERIALS AND METHODS

2.1 λ Red recombination method

Total genomic DNA of *V. furnissii* was isolated and purified. Small regions (about 200 bp in length) of the *nagE* gene were isolated, as well as the entire *cat* gene [from plasmid pKK232-8 (99)]. A transcriptional fusion was created by overlap extension PCR (100, 101). Plasmid pKD46, containing the λ Red recombinase system, was electroporated into *V. furnissii*. However, transformants containing the plasmid were not isolated, due to the fact that *V. furnissii* is resistant to ampicillin, the antibiotic used to select for transformants.

2.1.1 Preparation of *V. furnissii* genomic DNA

Genomic DNA was prepared using a Microbial DNA Isolation Kit (Mo Bio Laboratories) according to the enclosed protocol. Genomic DNA was visualized on a 0.8 % agarose gel shown in **Figure 14** on page 49.

2.1.2 Primer design

Vibrio furnissii strain NCTC 11218 was used in all experiments due to the recent publication of the organism's entire genome (89). The sequence for *nagE* can be found on the National Center for Biotechnology Information (NCBI) Online Nucleotide Database (Accession Number: U65014). The sequence for the plasmid pKK232-8 can be obtained from multiple sources, include the NCBI Online Nucleotide Database (102). The plasmid map and sequence located within BV Tech's database (103) was used to aid in visualization of the *cat* gene (encoding for the reporter protein, chloramphenicol acetyltransferase), located within the plasmid. The nucleotide sequence isolated includes all three start codons located within pKK232-8 (Accession Number: U13859) (104). Primers were handpicked from the genetic sequences, and were then examined for dimers, hairpins, and other parameters using NetPrimer® (105). Primer sequences are shown in **Table 1** on the following page. **Figures 11 and 12** on pages 36 and 37 display the location of the primers within their respective genes.

Table 1. Primer Sequences for overlap extension PCR

Gene	Primer	Oligo
nagE	F’	5’ – TTG CTA CTT TGC CTG CCG
	R’	5’ –CCG ACA AAC AAC AGA TAA AAA CAT ACA TAC ATA CGA GAC CAG CC
nagE	F’	5’ – CGC CTG AAT AAG TGA TAA TAA CTA TGA TGT TTG GTC TGC C
	R’	5’ – CTG AGA AAC CGA AAC CTG C
cat	F’	5’ – ATG TTT TTA TCT GTT GTT TGT CGG
	R’	5’ – ATT GAT GAA GCG TTA GCG GG

All primers were examined for dimers, hairpins, and other parameters using NetPrimer®, and synthesized by Eurofins Genomics.

Figure 11. Location of primers within *nagE*

1 aagcttttaa tttgcggagc aaaattaata tcataaactg agcctgacta aattgagcga
61 ctaaaataag tcgtccagtc caataatacc aaaatcctat agggggaact
111 taaggtgaat attcttggat attttcaaaa agtaggtaag gccctgatgg
161 tgcctg**ttgc tactttgcct gccg**cggcca ttcttatggg tgtcggctac
211 tggattgacc cgaatggttg gggtgcaaac tctgcattag caggcttcct
261 gattaaagcg ggtgcagcaa ttatcgacaa tatgtcatgg ttgtttgcag
311 tgggtgtcgc gtacggtatg tcgaaagaca aagacggcgc agcggcact
360 **g gctggtctcg tatgtatgta tgtt**gtgaca acgctactgt cacctggcgc
411 ggttgctcag attcaaggta tcgccgcctc tgaagttcca gcagcattta gcaaaattca
471 aaaccagttt gttggtatcc ttgtcggtat catctctgct gaaatttaca accgttactc
531 tgccgtcgaa ctgcacaaag cattggcgtt cttctcgggt aaacgtttgg ttccgatttt
591 gacatcattc gtcggtatcg tgctgtcttt tgtactgatg tacatctggc cagcaatcta
651 cggtggtctg gtgcactttg gtgaatcaat tcaaggcatg ggcgcaaccg gtgcaggtat
711 ctacgcattc tttaaccgcc tattgattcc tgttggccta caccacgcac tgaactcagt
771 attctggttc gacgtggcgg gcattaacga tattccgaac ttcctcggtg gtgctaaatc
831 tatcgcagaa ggtactggta ttgtcggtgt gacggggatg taccaagcgg gcttcttccc
891 a**atcatgatg tttggtctgc c**aggcgctgc gctagcgatg taccacacgt caacggcgaa
951 aaacaaagag aaagttgctg gtatcatgat cgctgctgca ttcgctgcgt tctttaccgg
1011 tgtgactgaa ccgctagaat tctcattcat gttcctagca ccaatgcttt acgttctgca
1071 cgcattgctg actggtatct ctgtattcat cgctgcatca atgcactgga
1121 tt**gcaggttt cggtttctca g**ctggtcttg tggatatggt actgtcatca cgtaacccac
1181 tggcggtgaa ctggtacatg ctgattgttc aaggtctggt gttctttacg ctgtactacg
1241 tgattttccg taccgttatc gtgaaattcg gtctgaaaac accgggtcgt gaagatgatg
1301 aagaaacaac gtctgcgaca aaaggttcga ctgagtcgtc tgaactggct aaacaatatc
1361 tgcaagttct gggtggtcac gacaacctgt ctaacatcga cgcgtgtatc actcgtcttc
1421 gtctgaccgt gaaagacatg tctatcatcg atgagaaaga gctgaaagcg ctgggcgcaa
1481 tgggtgttgt gaaactgggt tcaaacaacc ttcaagttat ccttggccca ctagctgaaa
1541 tcatcgcggg tcaaatgaag aacattcgca ctgaagagca cgtgacagaa gcaaaacagt
1601 cataagtcgc ttcaaacgcg agtccttacc aaagccttcg cctagtgcga aggctttttc
1661 gtctgatcgg tttggcgata tatccgccgt acaccagaaa taatcacaag aaaacggcag
1721 tttttattgt gaattcgttc agaattgtgg atcatggccg acaataattt ctgctctgcc
1781 gggcttttgt agcttttaaa tgcagaaaaa cttttctgac aatactaaat aaacttgagg
1841 tgctatagat gagtgaagct gaggctcgtc catcgaactt cattcgccaa atcattgata
1901 aagatttagc ggatggtaaa cacactagcg tgcatactcg tttcccacca gaacccaacg
1961 gttatctgca tatcgggcac gcgaagtcga tctgtttgaa ctttggtatt gctcaggact
2021 atcagggtca gtgtaactta cgttttgacg acacaaaccc agaaaaagaa gatctcgaat
2081 acgttgagtc gattaagaaa gatgtgaact ggttaggctt cgaatggtct ggcgacgtat
2141 gttactcatc tgattacttc gacaagcttt aatgcggtag

The upstream amplicon is 250 base pairs in length and the downstream amplicon is 218 base pairs in length.

Figure 12. Location of primers within *cat* gene

1 ttcccaggca tcaaataaaa cgaaaggctc agtcgaaaga ctgggccttt
51 cgt**tttatct gttgtttgtc gg**tgaacgct ctcctgagta ggacaaatcc
101 gccgggagcg gatttgaacg ttgcgaagca acggcccgga gggtggcggg
151 caggacgccc gccataaact gccagggaat tcccggggat ccgtcgacct
201 gcagccaagc t***tga***g***tag***ga caaatccgcc gagcttcgac gagattttca
251 ggagc***taa***gg aagc***taa***aat ggagaaaaaa atcactggat ataccaccgt
301 tgatatatcc caatcgcatc gtaaagaaca ttttgaggca tttcagtcag
351 ttgctcaatg tacctataac cagaccgttc agctggatat tacggccttt
401 ttaaagaccg taaagaaaaa taagcacaag ttttatccgg cctttattca
451 cattcttgcc cgcctgatga atgctcatcc ggaattccgt atggcaatga
501 aagacggtga gctggtgata tgggatagtg ttcacccttg ttacaccgtt
551 ttccatgagc aaactgaaac gttttcatcg ctctggagtg aataccacga
601 cgatttccgg cagtttctac acatatattc gcaagatgtg gcgtgttacg
651 gtgaaaacct ggcctatttc cctaaagggt ttattgagaa tatgtttttc
701 gtctcagcca atccctgggt gagtttcacc agttttgatt taaacgtggc
751 caatatggac aacttcttcg cccccgtttt caccatgggc aaatattata
801 cgcaaggcga caaggtgctg atgccgctgg cgattcaggt tcatcatgcc
851 gtctgtgatg gcttccatgt cggcagaatg cttaatgaat tacaacagta
901 ctgcgatgag tggcagggcg gggcgtaatt ***ttttta***ggc agttattggt
951 gcccttaaac gcctggtgct a**cgcctgaat aagtgataat a**agcggatga

The *cat* gene found within the plasmid pKK232-8 is promoterless. Important regulatory sequences including start codons and the termination sequence are contained within the amplicon. The amplicon is 942 base pairs in length.

2.1.3 Overlap Extension PCR

Overlap extension PCR was carried out to create a transcriptional fusion using FideliTaq polymerase (USB®) and the primers described above (100, 101). Optimal conditions for the primers were determined experimentally. Upstream and downstream segments of approximately 200 nucleotides in length were isolated from the genomic DNA of *V. furnissii*. The optimal annealing temperature and $MgCl_2$ concentrations for the upstream and downstream primer pairs were found to be 50°C and 1.5 mM and 47°C and 5.5 mM, respectively. The *cat* gene was isolated from plasmid pKK232-8. The optimal annealing temperature and $MgCl_2$ concentration for this primer pair were found to be 42°C and 3.5 mM.

2.1.4 CAT assay

A *FAST* Cat ® Chloramphenicol Acetyltransferase Assay Kit (Molecular Probes) was chosen to measure chloramphenicol acetyltransferase activity. An Infinite® Microplate reader (Tecan) housed in another laboratory on campus was chosen to measure fluorescence intensity.

2.1.5 Problems encountered

During the course of the study, it was observed that transformants were identical to the negative control on marine agar plate imbued with ampicillin. The literature was thoroughly examined for an explanation to this phenomenon, and *V. furnissii* was found to be resistant to ampicillin (106). It was determined, both according to the literature and by experimental observation that our strain of *V. furnissii* is susceptible to chloramphenicol and somewhat susceptible to kanamycin.

2.2 Quantitative PCR

Quantitative PCR (qPCR) was carried out in accordance with the Minimum Information for publication of Quantitative real-time PCR Experiments (MIQE) guidelines (107).

Primers were designed to target *nagE* (the gene of interest) and *gyrB* (a constitutively expressed reference gene). Total RNA was isolated, purified, and examined for integrity. First strand cDNA was synthesized by reverse transcription of total RNA using random hexamers. Expression data were collected by qPCR using gene specific primers, and these data were analyzed by one-way ANOVA with Tukey's post-hoc multiple comparisons using the latest Prism software (Graphpad™).

2.2.1 Primer design

Vibrio furnissii strain NCTC 11218 (Microbiologics®) was used in all experiments due to the recent publication of the organism's entire genome (89). The constitutively transcribed *gyrB* gene, encoding DNA gyrase subunit B, was chosen as a reference gene due to its stability in 7 different *V. cholerae* strains under salt stress conditions (108). The Primer-BLAST tool provided by the NCBI (109) was used to identify potential primers within *gyrB* (Accession Number: NC_0166202) and to evaluate for primer specificity. Primers previously designed for *nagE* were also used in this experiment (see section **2.1.2** on page 33 for more information). Potential primers were then examined for dimers, hairpins, and other parameters using NetPrimer® (Premier Biosoft) (105). An amplicon 298 base pairs in length was chosen. Primers were synthesized by Eurofins Genomics. Primers were suspended in TE buffer to a concentration of 50 pmol before use.

Table 2. Primer Sequences for Real-Time PCR

Gene	Primer	Oligo
nagE	F’	5’ – TTG CTA CTT TGC CTG CCG
	R’	5’ –CCG ACA AAC AAC AGA TAA AAA CAT ACA TAC ATA CGA GAC CAG CC
gyrB	F’	5’ – GAC GGT AGG TTT GGG TGT GC
	R’	5’ – ATT GAT GAA GCG TTA GCG GG

Primer specificity was verified *in silico* using Primer-BLAST (NCBI), and examined for dimers, hairpins, and other parameters *in silico* using NetPrimer®. All primers were synthesized by Eurofins Genomics.

Figure 13. Location of primers within control gene, *gyrB*

ORIGIN

1 ctacacgtcg aggttcgcca ctttcagggc gttgttttcg atgaacgcac gacgaggttc
61 aacttgatcc cccatcagtg tggtaaacag ctcatccgca cccacggcat catcgatggt
121 gacttgcatc atgcgacgtg tttctggatc catggtggtt tcccatagct gatccgggtt
181 catctcaccc aaacctttgt agcgctgtac agacaagcca cggcgtgatt ctttgatcag
241 ccaatcaagg gccgctgcaa agctcgccac cggttgtgta cgctcgccac gtttgatgta
301 tgcaccgtct tcgatcaggc catgcatcgc ttcagacaat tcagccagct tgccgtactc
361 tttggagttc agcagatcca cactcagcag gtattcgtgc gtcacaccgt gtgtgcgtac
421 tttgatgcgc ggtgagtaga cgttgtgttc cgcgttgtgt tccagcgtga agctgtattg
481 gctcgcgccc acttctttgg cgttcaactg atcaatcagt tgttgcgtcc acgcttgcgc
541 gccagcttca tcctgacatt tttcagccgt catgcgtggc atgtagatga attcatggat
601 cagagaatgc gggtaacgac ggctcatgcg ttcgatcagt ttgatggcag cattgtattg
661 ctgaaccaat ttctccaacg gtgcgcccgc caatgctggt gcgtcagcgt tcacgtgcag
721 ctctgcgttg tccatcgcca gtgcgatctg gtattggttc atcgcctctt catctttgat
781 gtactgctct tgtttgcctt tcttcacttt gtacaaaggt ggctgagcaa tgtagatgta
841 gccacgttca atcagctccg gcatttgacg gtagaagaac gttagcagca gcgtacgaat
901 gtgagaacca tcgacgtccg catcggtcat gatgatgatg ttgtggtaac gcagtttgtc
961 tgggttgtat tcgtcacggc cgataccgca gcccaacgct gtgatcagcg tggccacttc
1021 ttgcgacgac aacatcttgt caaaacgtgc tttttctacg ttaaggattt tacctttcag
1081 cggcagaatc gcctgattct tacggttacg accttgtttt gcagaaccgc ccgctgagtc
1141 accctccaca atgtagagtt cagacaacgc tggatctttt tcctgacagt ccgccagttt
1201 gccgggtagg cccgcgagat ccagtgcgcc tttacgacgt gtcatttcac gtgctttacg
1261 tgccgcttca cgcgcacgtg ctgcatcgat gattttgcta cacacgattt tcgcttccga
1321 tgggttttct gccaagaagt cattcaactt ctcgcccatg gccgattcaa ccgcagattt
1381 cacttctgaa gacaccagtt tgtctttggt ttggctcgag aattttggat caggcacttt
1441 caccgacacg accgccgtca acccttcacg cgcatcgtca cccgacgtcg cggttttggc
1501 tttcttggtg tagcattctt tgtccatgta agtgttcagt gtacgcgtta acgccgcacg
1561 gaaaccggcc aagtgcgtcc caccatcgcg ctgtggaatg ttgttggtga aacagtaaat
1621 gctttcttgg aaaccatcgt tccactgcat cgccacttcc acgctgatgc catcttcacg
1681 ttcagagttg aagtggaata ctttctcgtg gatgggcgtt ttgttgcggt tcaggtggtt
1741 tacaaacgct tgaataccgc cttcgtacat gaagtgatct tgtttgttgt cttcgcgctc
1801 atccaccagc ttgatggaca cgccagagtt caagaacgac agctcgcgca ggcgtttcgc
1861 cagaatttcg taatggaatt cgatgttggt aaaggtttca gcgcttggcc agaaacggac
1921 catggtgccg ctgcgatcgg tatcacccac caccgccaat ggcgcttcag gaacaccgt
1980 **gacggtaggtt tgggtgtgc**a ctttgccacc gcggtgaatg gtcaggacca ctttttccga
2041 cagggcgtta accaccgaca caccaacccc gtgcagacca ccggatactt tgtaggagtt
2101 gtcatcaaac ttaccaccgg cgtgcagaac cgtcatgatg acttctgccg cagacacttt
2161 ttcttcaggg tggagctcgg tcggaatacc acgaccgtca tcgctgaccg ataccgagtt
2221 atcttcgtga atggtcacga tgatgtcttt acagtaa**ccc gctaacgctt catcaat**cga
2281 gttatccacc acctcaaaaa ccatgtggtg cagaccggtg ccatcatcag tgtcgccgat
2341 gtacataccc ggacgcttac gtaccgcgtc tagacccttc agtactttaa tactcgatga
2401 atcgtaatta ttcgacat

2.2.2 Total RNA isolation and purification

Vibrio furnissii was cultured in Defined Minimal Media (110) containing either *N*-acetylglucosamine (GlcNAc), glucose (Glc), mannose (Man) (25mM), or lactate (50mM, to account for the racemic mixture of the substrate). GlcNAc is thought to be the inducer of the operon, glucose is an important PTS sugar, and mannose is another PTS sugar. Although lactate is an excellent carbon source for bacterial growth, it is not a sugar. In experiments studying chemotaxis in *V. furnissii*, swarming of the bacteria was not observed in the presence of lactate; swarming was observed when chitin oligomers were used as a nutrient source (16). Using lactate as an energy source should not induce of any phosphotransferase systems; therefore it was chosen to serve as a negative control. When the cultures reached an optical density of 0.3 at 600 nm (OD_{600} = 0.3), 3.0 mL of the culture was harvested and pelleted in a Microfuge® 22R Centrifuge (Beckman Coulter). These pellets were stored at -80°C for no more than 1 year before use.

Total RNA was isolated and purified from frozen pellets of *V. furnissii* using the E.Z.N.A.® Bacterial RNA Kit (Omega Bio-Tek, R6950-01) according to the enclosed protocol. Following isolation, contaminating DNA was removed from the samples using RQ1 RNase-free DNase (Promega). Purity and concentration of the RNA samples was determined using a NanoDrop ND-1000 Spectrophotometer (Ambion). Integrity of the RNA was determined by

visualization on a 5% household bleach (v/v) 1% agarose (w/v) gel (15). Isolated, purified RNA was stored at -80°C for no more than 1 year before use.

2.2.3 Reverse Transcription

A Verso cDNA synthesis kit (Thermo Scientific, #AB-1453/B) was used to create first strand cDNA from 500 ng of total RNA for each sample. This kit utilizes a unique Verso Reverse Transcriptase enzyme with significantly attenuated RNase H activity and an RT Enhancer buffer containing an enzyme that degrades genomic DNA at the beginning of the RT reaction for superior cDNA synthesis results. Reactions were carried out on a Mastercycler® gradient thermal cycler (Eppendorf) according to the protocol enclosed in the reverse transcription kit. Random hexamers were used to prime the RNA. Synthesized cDNA was stored at 4°C for no more than 1 month before use.

2.2.4 Quantitative PCR

The reactions were set up manually using VWR Signature™ Electronic pipettors (VWR, SE 10-1, SE 200-1) in 0.1 mL low profile, clear PCR 8-strip tubes with real-time caps (Axygen, 321-14-031). A C1000 Touch™ Thermal Cycler with a CFX96™ Real-Time System (Bio-Rad) was used to run qPCR. 2X Brilliant III SYBR® Green QPCR Master Mix (Agilent) was used for fluorescent detection of the PCR products. Data were analyzed using CFX Manager software

v. 3.1 (Bio-Rad), complementary to the CFX96^{TM} Real-Time System. Statistical significance was determined by one-way ANOVA with Tukey's post-hoc multiple comparisons ($\alpha = 0.05$) using the latest Prism software (Graphpad).

Table 3. Reverse Transcription Reaction Conditions

Reaction Reagents

Sample	500 ng
RT enzyme enhancer	1 µL
dNTPs	2 µL
5xRT buffer	4 µL
random hexamers	1 µL
RT enzyme mix	1 µL
Nuclease Free water	sufficient
Total Volume	20 µL

Thermal cycling Parameters

Step	Temp	Time
Primer extension	25°C	10 minutes
cDNA synthesis	42°C	30 minutes
Reaction termination	85°C	5 minutes
Chill	4°C	∞

Thermocycler lid held a 105°C.

Table 4. Real-Time PCR Reaction Conditions

Reaction Reagents

DI water	3 µL
5X buffer[2]	4 µL
Sample	1 µL
Fwd primer	1 µL
Rev primer	1 µL
2X SYBR Mastermix	10 µL
Total Volume	20 µL

Thermal cycling Parameters

Step	Temp	Time
1. Initial Denaturation	95°C	3 minutes
2. Denaturation	95°C	30 seconds
3. Annealing and Elongation	60°C	30 seconds
4. Plateread		
5. Go to 2, 54 x's		
6. Initial melt curve temp	65°C	31 seconds
7. Gradient melt curve increments	65°C+0.5°C/cycle	5 seconds
8. Plateread		
9. Go to 7, 60 x's		

Thermocycler lid held a 105°C.

2. Details concerning 5X Buffer:
   Made in-house, original composition developed by Cephied.

   1 mg/ml Bovine Serum Albumin (BSA)
   750mM Trehalose
   1% Tween-20

CHAPTER 3

RESULTS

3.1 λ Red recombination method

Genomic DNA was successfully isolated from *V. furnissii* NCTC11218 as shown in **Figure 14** on page 48.The targeted fragments were successfully isolated from genomic DNA, as depicted in **Figure 15** on page 49. These fragments were used to create the desired transcriptional fusion by overlap extension PCR as shown in **Figure 16** on page 50. However, we were unable to isolate transformants contaminating the plasmid necessary for λ Red recombination due to the natural resistance of *V. furnissii* to ampicillin (data not shown).

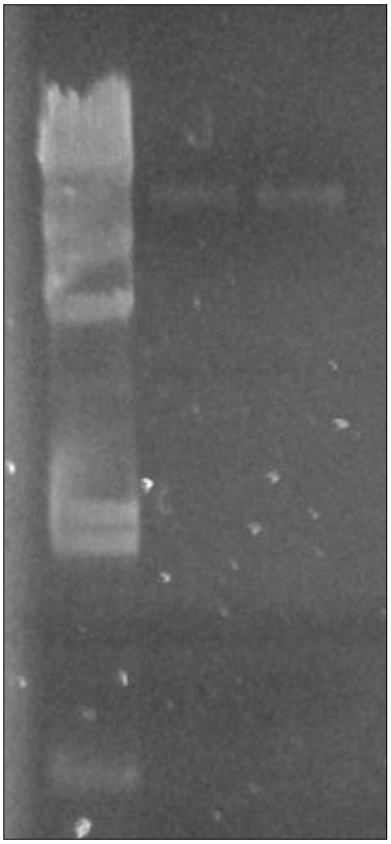

High MW DNA

Lane	Sample
1	λHindIII ladder
2	genomic DNA, sample 1
3	genomic DNA, sample 2

Figure 14. Genomic DNA of *V. furnissii.*
The presence of a single band of high molecular weight DNA indicates that genomic DNA was successfully isolated without contaminating fragments or naturally occurring plasmids.

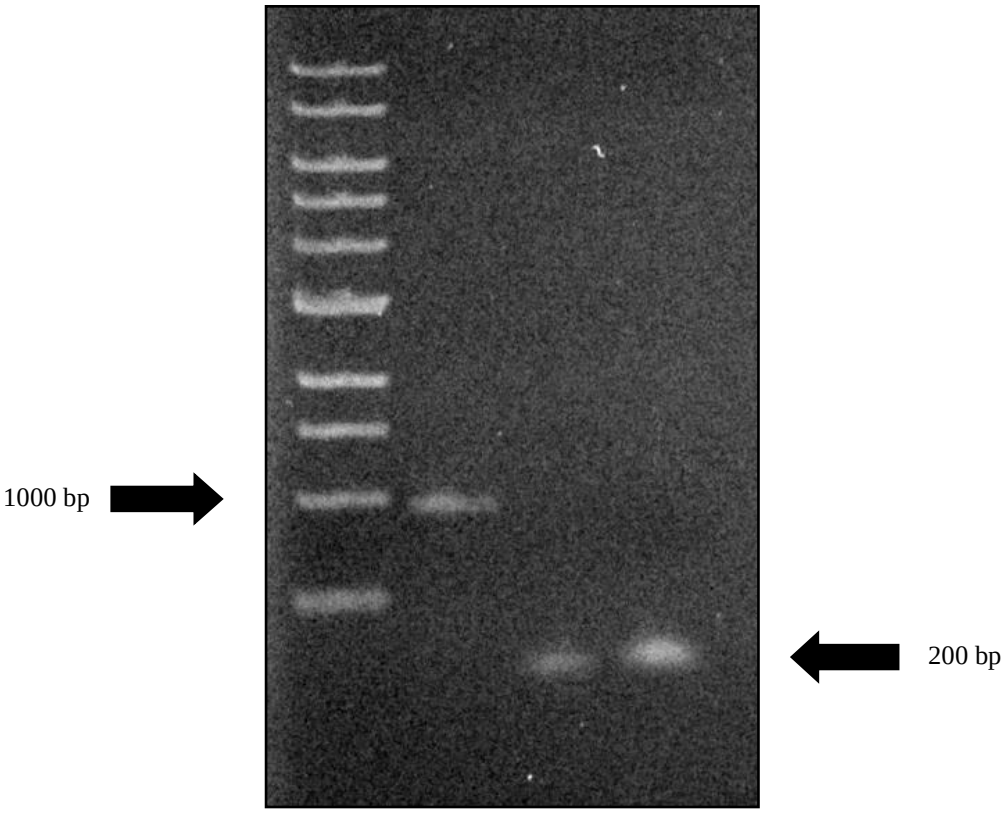

Figure 15. Isolated DNA fragments.

Lane	Sample
1	standard ladder
2	*cat* gene ~1000 bp
3	190-408*nagE* ~200 bp
4	919-1165*nagE* ~200 bp

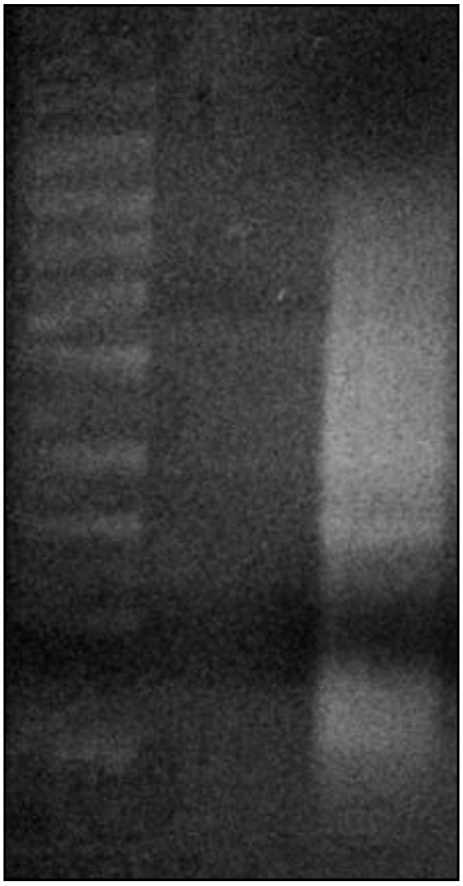

1500 bp

Lane	Sample
1	standard ladder
2	empty
3	Overlap extension PCR Product

Figure 16. Transcriptional fusion product.
What is presumed to be the 190-408*nagE-cat*-919-1165*nagE* transcriptional fusion product can be seen in lane 3. Non-specific products are also observed (smearing). The identity of this transcriptional fusion product was not confirmed by sequencing techniques.

3.2 RNA and qPCR assays

Primers were analyzed *in silico* prior to ordering. RNA integrity and purity was verified following RNA isolation. Validation and quantification data were collected simultaneously.

3.2.1 *In silico* analyses of primers

When analyzed using the Primer-BLAST tool on the NCBI website, the primer pair targeting *gyrB* was found to have one intended target with a length of 298 base pairs and no potential unintended targets within the genome of *V. furnissii* NCTC 11218. The primer pair targeting *nagE* was found to have one intended target with a length of 250 base pairs and one potential unintended target with a length of 3355 base pairs within the genome of the organism (data not shown).

3.2.2 Purity of RNA

Purity of RNA is based on spectrophotometric absorbance ratios of A_{260}:A_{280} and A_{260}:A_{230}, with ideal ratios being ~1.8-2.0 and ~1.8-2.2 respectively. An A_{260}:A_{280} ratio between ~1.8 and ~2.0 indicate that the sample is devoid of protein contaminants. A_{260}:A_{230} absorbance ratios appreciably lower than 1.8 may indicate the presence of co-purified salt contaminants. Total RNA isolated was found to be acceptably pure. See **Table 5** on page 54 for data.

3.2.3 Integrity of RNA

Integrity of RNA can be tested by visualization on a denaturing agarose gel (15). Observation of two bright, tight bands representing the greater and smaller ribosomal subunits, with the greater subunit having an intensity of about twice that of the smaller subunit, is generally accepted to indicate intact RNA. Samples of total RNA isolated were visualized on a 5% household bleach (v/v) 1% agarose (w/v) gel and found to have acceptable integrity. See **Figure 17** on page 55 for details.

3.2.4 Validation data

Validation data for qPCR assays include *in situ* demonstration of primer specificity and reaction efficiency. Ideal specificity can be demonstrated by a single peak in the melt curve. Efficacy of the reaction indicates the rate at which the polymerase converts reagents to product. Ideal reaction efficiency is 90-110%. Additionally, the coefficient of determination (r^2) can be used to evaluate the optimization of the assay. An r^2 value of > 0.980 demonstrates linearity of the standard curve and ultimately gives an indication of variability across assay replicates (17). Melt curves and standard curves for both sets of primers are shown in **Figures 18 and 19** on pages 56 and 57.

3.2.5 Quantification data

Transcription of *nagE* was up-regulated in the presence of GlcNAc only, as shown in **Figure 20** on page 58. There appears to be some down-regulation of the expression of *nagE* in the presence of glucose only (not statistically significant).

Table 5. Absorbance Ratios for total RNA

Sample	A_{260}:A_{280}
GlcNAc	
1	2.11
2	2.05
3	2.11
4	2.04
5	2.10
6	2.07
Glc	
1	2.06
2	2.04
3	2.01
4	2.10
5	2.09
6	2.04
Man	
1	2.06
2	2.04
3	2.11
4	2.08
5	2.10
6	2.06
Lactate	
1	2.06
2	2.11
3	2.10
4	2.04
5	2.05
6	2.06

Purity of RNA is based on spectrophotometric absorbance ratios of A_{260}:A_{280} with acceptable ratios being ~1.8-2.0. The A_{260}:A_{280} ratios for all samples are ~2.0, indicating that the samples are reasonably devoid of protein contaminants.

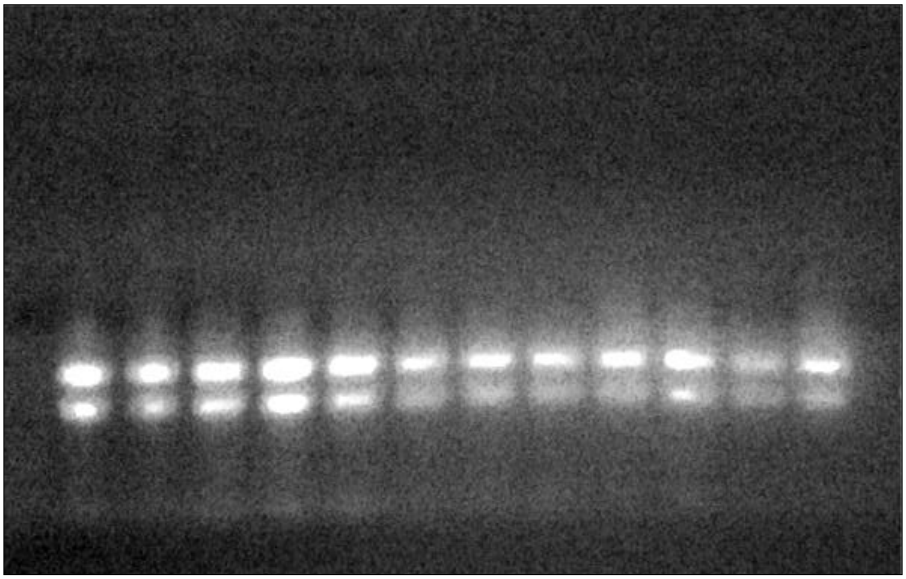

Figure 17. Agarose bleach gel. Note the bright, tight bands representing ribosomal subunits 50S and 30S. The intensity of the 50S band is about twice that of the 30S band. The presence of these bands indicates that the ribosomal RNA is intact and therefore mRNA is also of good integrity (15).

gyrB

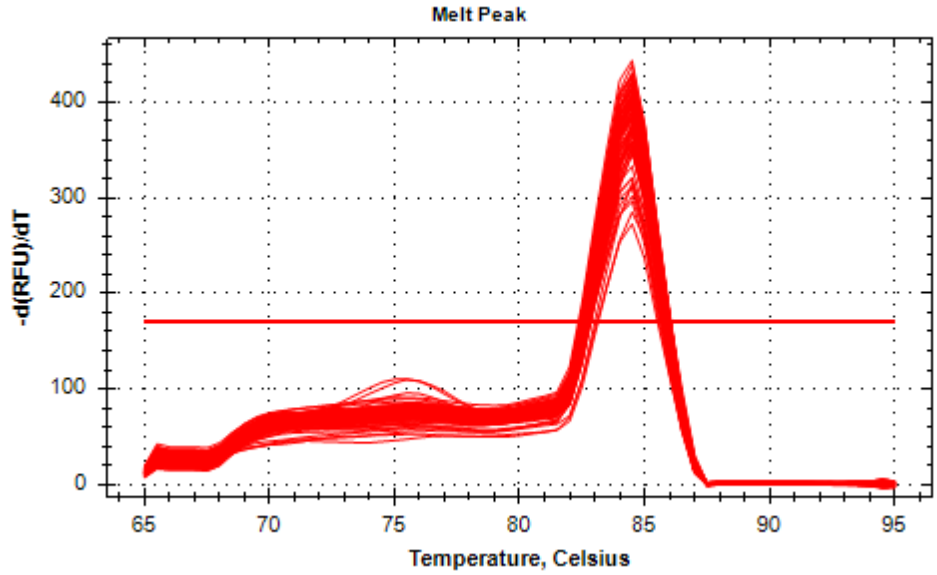

nagE

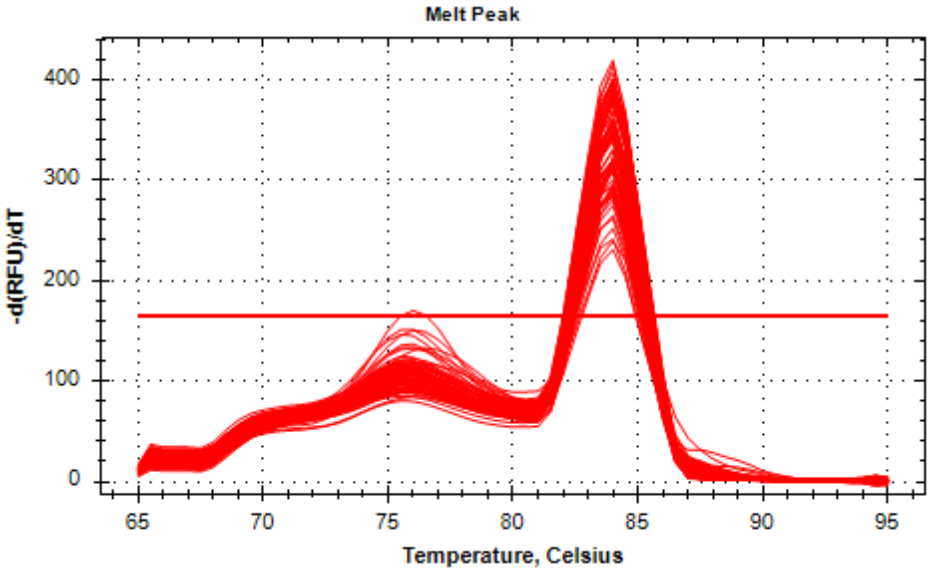

Figure 18. Melt curve peaks for both sets of primers. A single peak on the melt curve indicates a single product for a pair of PCR primers. Some artifact is observed in both melt curves, but these were assumed to affect all samples with relatively little variability.

gyrB

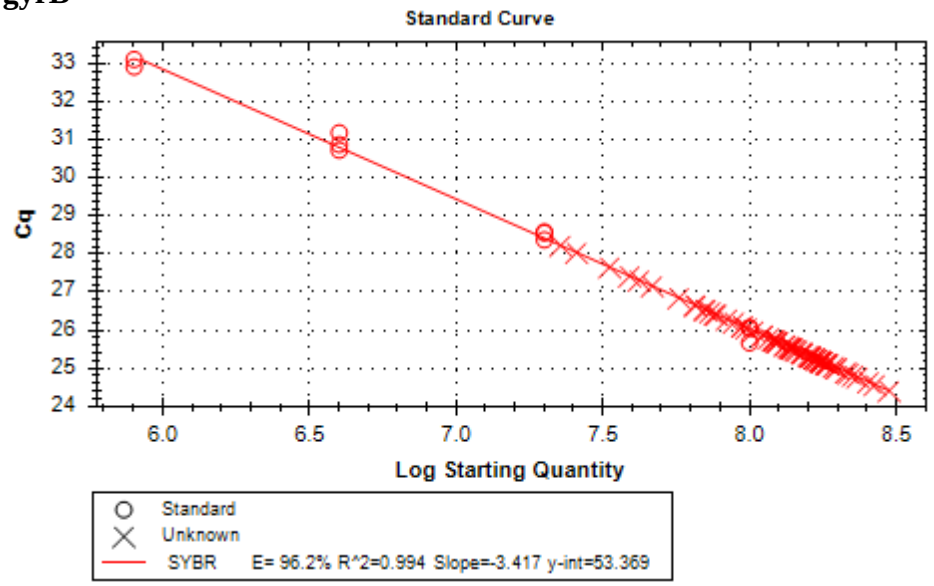

nagE

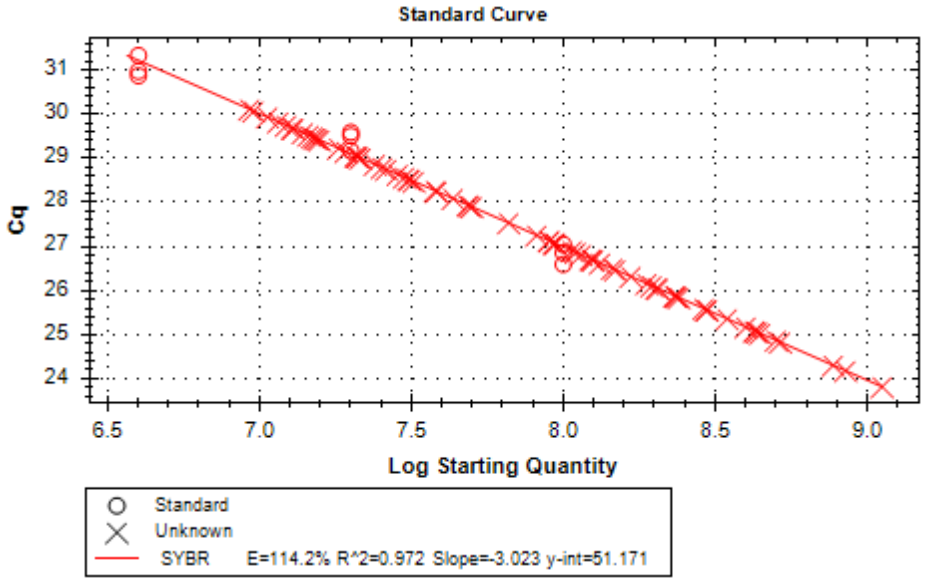

Figure 19. Standard curve data for both sets of primers. E = efficacy in this figure. Recall that ideal efficacies range from ~90-110%, and that an $r^2 > 0.980$ is considered desirable (17).

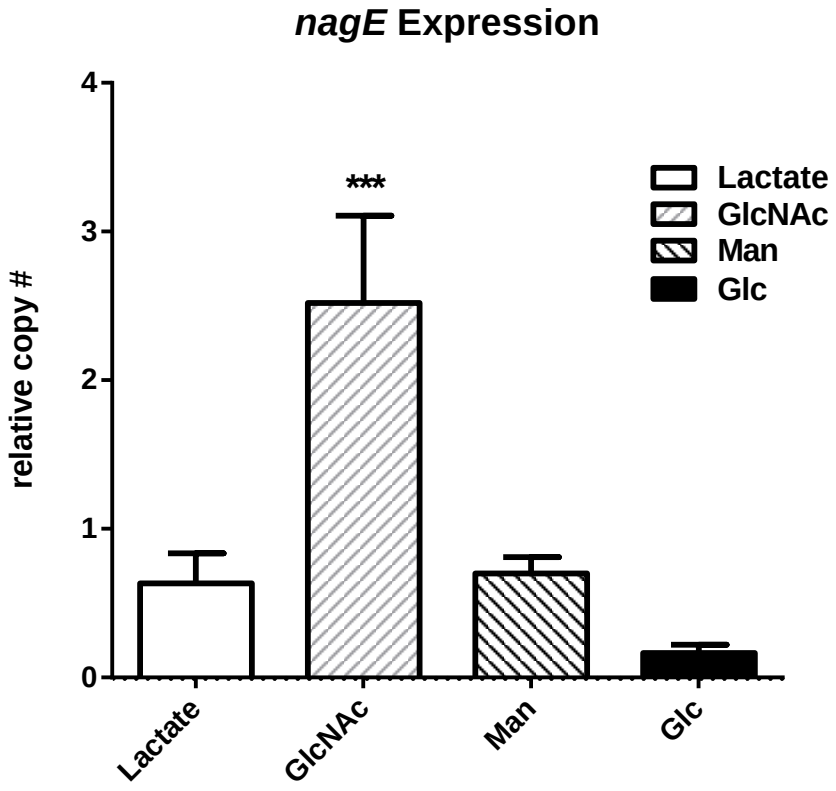

Figure 20. Expression Data. All comparisons are relative to Lactate. Data Analysis was carried out by one-way ANOVA with post-hoc multiple comparisons (Tukey's Test, $\alpha = 0.05$).

Error bars represent Mean +/- S.E.M. N = 6

*** = $p<0.0001$

CHAPTER 4

DISCUSSION

4.1 Comparison of methods

It has been established that quantification of mRNA does not necessarily equate to protein expression within complex samples such as cellular lysates (111-114). Furthermore, no real-time thermal cycler was available for our lab to use at the beginning of this study. Therefore, a homologous recombination method was first chosen to study protein expression for this project. However, due to the complex nature of the method and natural antibiotic resistance, we were unable to collect data using the λ Red recombination method at this time. Data may still be collected in our lab via this method at a later date after the method has been properly modified. Modification of this method may take a substantial time commitment from another student.

West Texas A&M University recently gained access to a real-time thermal cycler and nanodrop spectrophotometer. Collaboration among three laboratories (belonging to Drs. Bouma, Byers, and Karaganis) has made it possible to collect the desired data within a reasonable time-frame, less than two years after the decision to change methods was made.

Each method has its advantages and pitfalls. Reverse transcription followed by quantification of mRNA is relatively simple, easily reproduced, and generates data which lends itself to statistical analyses. In fact, one driving force behind the popularity of RT qPCR methods has been the preference of quantifiable molecular data to support phenotypic observation (17). However, it is not an entirely accurate representation of protein expression. On the other hand, using a homologous recombination method to insert a reporter gene into the gene of interest in order to measure enzymatic activity gives a closer representation of protein expression levels. However, the methods are much more complex and may involve additional sources of experimental error.

4.1.1 λ Red recombination

Many labs have quantified gene expression in different bacteria by inserting a "reporter gene" into a target gene and measuring amount of protein produced by the reporter gene (115, 116). A reporter gene is a gene whose protein product can be simply, yet accurately, measured. A transcriptional fusion can be constructed by overlap extension PCR (100, 101). The reporter gene can then be inserted into the gene of interest within the chromosome of the organism using the Red recombinase system isolated from the phage λ (115-118). Following insertion, expression of the reporter gene can be measured under different growth conditions to determine which conditions lead in increased expression.

We chose to quantify the expression of *nagE* because inserting a reporter gene into the chromosome will not affect transcription of *nagC*, the gene encoding the hypothetical regulatory protein of the *nag* operon. This method is considered an *in vivo* demonstration because it takes place within the living organism. *In vivo* demonstrations often give a better depiction of intracellular processes than *in vitro* demonstrations, which take place in controlled, artificial environments.

4.1.2 Reverse transcription followed by real-time quantitative PCR

The reverse transcriptase (RT) enzyme (initially dubbed RNA-dependent DNA polymerase) was independently discovered by Howard Temin and David Baltimore in virions in 1970 (119, 120). Two years later, the Baltimore laboratory demonstrated that purified RT was capable of synthesizing complementary DNA from cellular mRNA (121), a finding which had remarkable implications for the field of molecular biology.

Roughly 20 years later, the quantitative potential of reverse transcription followed by PCR was realized (122) and, several labs utilized the procedure to quantify gene expression (123-127). Soon, the importance of using an internal control was demonstrated (128, 129). Within another decade, the need for prudent selection of a stable internal control gene for accurate normalization was addressed (130, 131), and concerns regarding the reliability of data obtained by

such a method were beginning to emerge (132). At least one retraction of a "major finding" in 2005 caused some alarm within the scientific community (133). Stephen Bustin was one of the most notable scientists to emerge from those calling for a reform in the reporting of data generated by RT qPCR (132, 134-140). He led a group of scientists in the publication of the Minimum Information for Publications of Quantitative Real-Time PCR Experiment (107) concurrently with publication of Real Time PCR Data Markup Language (RDML)[3]. These guidelines, widely accepted as the current standard for the field, assist the reader in her ability to critically analyze reported data.

The integrity and purity of mRNA have been shown to have an effect on the reliability and reproducibility of reverse transcription (107, 141). Several different methods to assess integrity and purity of mRNA were examined (15, 17, 142, 143). The Agarose Bleach Gel method was chosen due to its safety, simplicity, and cost effectiveness.

Not many reference genes exist or are known for prokaryotes, a problem also encountered in the study of many plant species (144). Only one paper was found reporting results regarding stability of potential internal control genes within the genus *Vibrio* (108).

3. The paper for RDML was published by another group of scientists led by Lefever in a separate journal (14).

4.2 Significance of Findings

Transcription of *nagE* has been shown to be up-regulated in the presence of GlcNAc. Interestingly, transcription of *nagE* appears to be down-regulated in the presence of glucose, although these findings are not statistically significant. It is tempting to speculate that regulation of the *nag* operon may depend on the phosphorylation state of the protein subunits necessary for transport via the glucose specific permease, such as $EIICB^{Glc}$ or $EIIA^{Glc}$. Although the operator region for *nagE* has been shown to bind more tightly to Mlc than NagC *in vitro* (72), and analysis of the *V. furnissii* genome suggests that the organism does possess an *mlc* gene, it seems unlikely that Mlc is involved in the regulation of *nagE* in the presence of glucose *in vivo*. Down-regulation of *nagE* transcription in the presence of glucose suggests that this operon is not regulated by Mlc in the same manner as *manXYZ*. In the presence of glucose, *manXYZ* is actually up-regulated due to the sequestration of Mlc to desphophorylated $EIICB^{Glc}$ (92, 95). This results in an increase in the number of transporters whereby glucose can enter the cytoplasm. Since NagE also transports glucose, it is not clear why expression of *nagE* would be repressed in the presence of glucose.

It seems more likely that expression of *nagE* is affected by the phosphorylation state of $EIIA^{Glc}$. The transport and phosphorylation of GlcNAc by EII^{Nag} has been shown to be dependent on the presence of $P\sim EIIA^{Glc}$ in *V. fischeri*; however, CRP-cAMP activity is not suppressed in the presence of GlcNAc as it is in the presence of glucose (145) . The nuances of regulation of metabolism by $EIIA^{Glc}$ and the CRP-cAMP complex

are not well understood. The *crr* gene encoding the soluble $EIIA^{Glc}$ protein in *V. furnissii* has previously been isolated and sequenced by our lab (146), but protein purification and exhaustive biochemical studies remain to be carried out.

4.3 Future directions

These data represent a gene expression study. Protein expression studies to confirm the qPCR results remain to be carried out.

Future studies could also include further characterization of the *nag* operon and other PTS operons. For instance, it would be interesting to investigate the putative binding of NagC to the control region of the *nag* operon. A histidine tag would need to be attached to NagC in order to purify and study the protein. Similarly, analysis of the genome of *V. furnissii* suggests that an *mlc* gene (encoding the protein Mlc) exists (Accession Number: WP_014204688); however, this protein is categorized as a putative "transcriptional regulator" on NCBI, and no biochemical studies have been carried out on this protein. It would be interesting to study the role of this important regulatory protein in *V. furnissii*.

Currently there is only one paper which reports results regarding the stability of potential internal control genes in *V. cholerae* (108). It would be meaningful and worthwhile to examine the stability of several potential reference genes in *V. furnissii*, strain NCTC 11218.

A *ptsG* homologue in *V. furnissii* has been identified through DNA complementation studies (88, 89), but protein purification and other biochemical assays remain to be carried out.

Due to the availability of necessary equipment as well as the expertise of Drs. Bouma, Byers, and Karaganis, a myriad of other prokaryotic gene expression studies are now available to students attending West Texas A&M University who possess sufficient initiative and drive to carry them out.

REFERENCES

1. **Voet D, Voet JG.** 2011. Biochemistry, 4th ed. John Wiley & Sons, Hoboken, NJ.
2. **U.S. D.O.E.** 2008. Carbon Cycling and Biosequestration: Report from the March 2008 Workshop. Oak Ridge National Laboratory. https://public.ornl.gov/site/gallery/gallery.cfm?citation=24. Accessed December 10th, 2016.
3. **CNX OpenStax.** Microbiology, v. 4.4. Creative Commons Licence Attribution 4.0 International. Published Online. https://cnx.org/contents/5CvTdmJL@4.4:W1kvc5fi@4/Unique-Characteristics-of-Prok. Accessed April 20th, 2017.
4. **Purves WK, Sadava D, Orians GH, Heller HC.** 2001. Life, the science of biology, 6th ed. Sinauer Associates, Sunderland, MA.
5. **Fenchel T, King G, Blackburn TH.** 1998. Bacterial biogeochemistry : the ecophysiology of mineral cycling. Academic Press, San Diego, CA.
6. **Dahl, J.** 2008. Gram-negative cell wall. Creative Commons Licence Attribution-Share Alike 4.0 International. WikiMedia Commons, Published Online. https://en.wikipedia.org/wiki/File:Gram_negative_cell_wall.svg. Accessed on April 20th, 2017.

7. **Berg IA, Kockelkorn D, Buckel W, Fuchs G.** 2007. A 3-hydroxypropionate/4-hydroxybutyrate autotrophic carbon dioxide assimilation pathway in Archaea. Science **318:**1782-1786.

8. **Evans MC, Buchanan BB, Arnon DI.** 1966. A new ferredoxin-dependent carbon reduction cycle in a photosynthetic bacterium. Proc Natl Acad Sci USA **55:**928-934.

9. **Herter S, Fuchs G, Bacher A, Eisenreich W.** 2002. A bicyclic autotrophic CO2 fixation pathway in *Chloroflexus aurantiacus*. J Biol Chem **277:**20277-20283.

10. **Huber H, Gallenberger M, et al.** 2008. A dicarboxylate/4-hydroxybutyrate autotrophic carbon assimilation cycle in the hyperthermophilic Archaeum Ignicoccus hospitalis. Proc Natl Acad Sci USA **105:**7851-7856.

11. **Ljungdahl LG.** 2009. A life with acetogens, thermophiles, and cellulolytic anaerobes. Annu Rev Microbiol **63:**1-25.

12. **Ljungdahl L, Wood HG.** 1965. Incorporation of C14 from Carbon Dioxide into Sugar Phosphates, Carboxylic Acids, and Amino Acids by *Clostridium thermoaceticum*. J Bacteriol **89:**1055-1064.

13. **Zarzycki J, Brecht V, Muller M, Fuchs G.** 2009. Identifying the missing steps of the autotrophic 3-hydroxypropionate CO2 fixation cycle in *Chloroflexus aurantiacus*. Proc Natl Acad Sci USA **106:**21317-21322.

14. **Lefever S, et al.** 2009. RDML: structured language and reporting guidelines for real-time quantitative PCR data. Nucleic Acids Res **37:**2065-2069.

15. **Aranda PS, LaJoie DM, Jorcyk CL.** 2012. Bleach gel: a simple agarose gel for analyzing RNA quality. Electrophoresis **33:**366-369.

16. **Keyhani NO, Roseman S.** 1999. Physiological aspects of chitin catabolism in marine bacteria. Biochim Biophys Acta **1473:**108-122.

17. **Taylor S, Wakem M, Dijkman G, Alsarraj M, Nguyen M.** 2010. A practical approach to RT-qPCR-Publishing data that conform to the MIQE guidelines. Methods **50:**S1-S5.

18. **Jodelet/Lépinay.** 2006. *Lyristes plebejus,* Cicada, leaving its moult. Creative Commons Licence Attribution-Share Alike 2.0 France. WikiMedia Commons, Published Online. https://commons.wikimedia.org/wiki/File:Lyristes_plebejus.jpg. Accessed on April 20th, 2017.

19. **Postma PW, Lengeler JW, Jacobson GR.** 1993. Phosphoenolpyruvate:carbohydrate phosphotransferase systems of bacteria. Microbiol Rev **57:**543-594.

20. **Galinier A, Deutscher J.** 2017. Sophisticated Regulation of Transcriptional Factors by the Bacterial Phosphoenolpyruvate: Sugar Phosphotransferase System. J Mol Biol doi:10.1016/j.jmb.2017.02.006.

21. **Hillewaert H.** 2005. *Cancer pagurus*. Vienna University of Technology, Creative Commons License CC BY-NC-ND 3.0, Vienna University of Technology

22. **Lal R.** 1995. Soils and global change. Lewis Publishers, Boca Raton, FL.

23. **Monod J.** 1949. The growth of bacterial cultures. Annu Rev Microbiol **3:**371-394.

24. **Pecan EV, Woodwell GM, Laboratory. BN.** 1973. Carbon and the biosphere; proceedings of the 24th Brookhaven symposium in biology.

doi:10.5962/bhl.title.4036. Technical Information Center, U.S. Atomic Energy Commission, Upton, N.Y.

25. **Bauman RW, Primm TP, Machunis-Masuoka E.** 2017. Microbiology, with diseases by taxonomy, 5th ed. Pearson, Boston, MA.

26. **Coico R.** 2005. Gram Staining, Current Protocols in Microbiology. John Wiley & Sons, Hoboken, NJ.

27. **Matias VR, Beveridge TJ.** 2005. Cryo-electron microscopy reveals native polymeric cell wall structure in *Bacillus subtilis* 168 and the existence of a periplasmic space. Mol Microbiol **56:**240-251.

28. **Zuber B, Haenni M, et al.** 2006. Granular layer in the periplasmic space of Gram-positive bacteria and fine structures of *Enterococcus gallinarum* and *Streptococcus gordonii* septa revealed by cryo-electron microscopy of vitreous sections. J Bacteriol **188:**6652-6660.

29. **Umeda A, Yokoyama S, Arizono T, Amako K.** 1992. Location of peptidoglycan and teichoic acid on the cell wall surface of *Staphylococcus aureus* as determined by immunoelectron microscopy. J Electron Microsc **41:**46-52.

30. **Bauman RW, Machunis-Masuoka E, Tizard IR.** 2004. Microbiology. Pearson/Benjamin Cummings, San Francisco, CA.

31. **Diseases NIoAaI.** 2014. Antibacterial Resistance Program Current Status and Future Directions. National Institute of Health, Bethesda, MD.

32. **Ventola CL.** 2015. The antibiotic resistance crisis: part 1: causes and threats. Pharm & Thera **40:**277-283.

33. **Ventola CL.** 2015. The antibiotic resistance crisis: part 2: management strategies and new agents. Pharm & Thera **40:**344-352.

34. **Peters NK, Dixon DM, Holland SM, Fauci AS.** 2008. The research agenda of the National Institute of Allergy and Infectious Diseases for antimicrobial resistance. J Infect Dis **197:**1087-1093.

35. **Gonil P, Sajomsang W.** 2012. Applications of magnetic resonance spectroscopy to chitin from insect cuticles. Int J Biol Macromol **51:**514-522.

36. **Jeuniaux C, Florkin M, Stotz EH.** 1971. Chitinous structures, p 595-632, Comprehensive biochemistry Volume 26 Part C. Elsevier, Amsterdam, Netherlands.

37. **Muzzarelli R.** 1977. Chitin. Pergamon Press, Oxford, England.

38. **Skjak-Braek G, Anthonsen T, Sandford P.** 1989. Chitin and Chitosan: Sources, Chemistry, Biochemistry, Physical Properties and Applications: Proceedings from the 4th International Conference on Chitin and Chitosan Held in Trondheim, Norway, August 22-24 1988. Elsevier applied science.

39. **Johnstone J.** 1908. Conditions of life in the sea: a short account of quantitative marine biological research. University Press, Cambridge, UK.

40. **Zobell CE, Rittenberg SC.** 1938. The occurrence and characteristics of chitinoclastic bacteria in the sea. J Bacteriol **35:**275.

41. **Brenner DJ, Hickman-Brenner FW, et al.** 1983. *Vibrio furnissii* (formerly aerogenic biogroup of *Vibrio fluvialis*), a new species isolated from human feces and the environment. J Clin Microbiol **18:**816-824.

42. **Yu C, Lee AM, Bassler BL, Roseman S.** 1991. Chitin utilization by marine bacteria. A physiological function for bacterial adhesion to immobilized carbohydrates. J Biol Chem **266:**24260-24267.

43. **Meadow ND, Revuelta R, Chen VN, Colwell RR, Roseman S.** 1987. Phosphoenolpyruvate:glycose phosphotransferase system in species of Vibrio, a widely distributed marine bacterial genus. J Bacteriol **169:**4893-4900.

44. **Keyhani NO, Li XB, Roseman S.** 2000. Chitin catabolism in the marine bacterium *Vibrio furnissii*. Identification and molecular cloning of a chitoporin. J Biol Chem **275:**33068-33076.

45. **Keyhani NO, Roseman S.** 1996. The chitin catabolic cascade in the marine bacterium *Vibrio furnissii*. Molecular cloning, isolation, and characterization of a periplasmic chitodextrinase. J Biol Chem **271:**33414-33424.

46. **Keyhani NO, Roseman S.** 1996. The chitin catabolic cascade in the marine bacterium *Vibrio furnissii*. Molecular cloning, isolation, and characterization of a periplasmic beta-*N*-acetylglucosaminidase. J Biol Chem **271:**33425-33432.

47. **Bouma CL, Roseman S.** 1996. Sugar transport by the marine chitinolytic bacterium *Vibrio furnissii*. Molecular cloning and analysis of the glucose and N-acetylglucosamine permeases. J Biol Chem **271:**33457-33467.

48. **Keyhani NO, Wang LX, Lee YC, Roseman S.** 1996. The chitin catabolic cascade in the marine bacterium *Vibrio furnissii*. Characterization of an *N,N'*-diacetyl-chitobiose transport system. J Biol Chem **271:**33409-33413.

49. **Pruzzo C, Huq A, Colwell RR, Donelli G.** 2005. Pathogenic Vibrio species in the marine and estuarine environment, p 464. *In* Belkin S, Colwell RR (ed),

Oceans and Health : Pathogens in the Marine Environment. Springer, Science and Business Media, New York, NY.

50. **Kohn GC.** 2008. Encyclopedia of plague and pestilence : from ancient times to the present, 3rd ed. Facts On File, New York, NY.

51. **Ali M, Lopez AL, You YA, Kim YE, Sah B, Maskery B, Clemens J.** 2012. The global burden of cholera. Bull World Health Organ **90:**209-218A.

52. **Meibom KL, Li XB, Nielsen AT, Wu CY, Roseman S, Schoolnik GK.** 2004. The *Vibrio cholerae* chitin utilization program. Proc Natl Acad Sci USA **101:**2524-2529.

53. **Lux TM, Lee R, Love J.** 2014. Genome-wide phylogenetic analysis of the pathogenic potential of *Vibrio furnissii*. Front Microbiol **5:**435.

54. **Quah SR.** 2016. International encyclopedia of public health, 2nd Edition. Academic Press, Kidlington, England.

55. **Daniels NA, Shafaie A.** 2000. A review of pathogenic Vibrio infections for clinicians. Infec Med **17:**665-685.

56. **Derber C, Coudron P, et al.** 2011. *Vibrio furnissii*: an Unusual Cause of Bacteremia and Skin Lesions after Ingestion of Seafood. J of Clin Microbiol **49:**2348-2349.

57. **Association ABS.** 2016. Risk Group Database.

58. **Kundig W, Ghosh S, Roseman S.** 1964. Phosphate Bound to Histidine in a Protein as an Intermediate in a Novel Phospho-Transferase System. Proc Natl Acad Sci USA **52:**1067-1074.

59. **Egan JB, Morse ML.** 1965. Carbohydrate transport in *Staphyloccus aureus* I. Genetic and biochemical analysis of a pleiotropic transport mutant. Biochim Biophys Acta **97:**310-319.

60. **Egan JB, Morse ML.** 1966. Carbohydrate transport in *Staphylococcus aureus* III. Studies of the transport process. Biochim Biophys Acta **112:**63-73.

61. **Egan JB, Morse ML.** 1965. Carbohydrate transport in *Staphylococcus aureus* II. Characterization of the defect of a pleiotropic transport mutant. Biochim Biophys Acta **109:**172-183.

62. **Murphey WH, Rosenblum ED.** 1964. Genetic recombination by transduction between mannitol-negative mutants of *Staphyloccous aureus*. Proc Soc Exp Biol Med **116:**544-548.

63. **Murphey WH, Rosenblum ED.** 1964. Mannitol catabolism by Staphyloccous aureus. Arch Biochem Biophys **107:**292-297.

64. **Doudoroff M, Hassid WZ, et al.** 1949. Direct utilization of maltose by Escherichia coli. J Biol Chem **179:**921-934.

65. **Postma PW, Roseman S.** 1976. The bacterial phosphoenolpyruvate: sugar phosphotransferase system. Biochim Biophys Acta **457:**213-257.

66. **Bertram R, Rigali S, Wood N, Lulko AT, Kuipers OP, Titgemeyer F.** 2011. Regulon of the *N*-acetylglucosamine utilization regulator NagR in *Bacillus subtilis*. J Bacteriol **193:**3525-3536.

67. **Bouma CL, Roseman S.** 1996. Sugar transport by the marine chitinolytic bacterium *Vibrio furnissii*. Molecular cloning and analysis of the mannose/glucose permease. J Biol Chem **271:**33468-33475.

68. **Deutscher J, Francke C, Postma PW.** 2006. How phosphotransferase system-related protein phosphorylation regulates carbohydrate metabolism in bacteria. Microbiol Mol Biol Rev **70:**939-1031.

69. **Erni B, Zanolari B.** 1985. The mannose-permease of the bacterial phosphotransferase system. Gene cloning and purification of the enzyme IIMan/IIIMan complex of *Escherichia coli*. J Biol Chem **260:**15495-15503.

70. **Erni B, Zanolari B, Kocher HP.** 1987. The mannose permease of *Escherichia coli* consists of three different proteins. Amino acid sequence and function in sugar transport, sugar phosphorylation, and penetration of phage lambda DNA. J Biol Chem **262:**5238-5247.

71. **Plumbridge J, Kolb A.** 1991. CAP and Nag repressor binding to the regulatory regions of the *nagE-B* and *manX* genes of *Escherichia coli*. J Mol Biol **217:**661-679.

72. **Plumbridge J.** 2001. DNA binding sites for the Mlc and NagC proteins: regulation of *nagE,* encoding the N-acetylglucosamine-specific transporter in *Escherichia coli*. Nucleic Acids Res **29:**506-514.

73. **Plumbridge J.** 1987. Organisation of the *Escherichia coli* chromosome between genes *glnS* and *glnU, V.* Mol Gen Genet **209:**618-620.

74. **Plumbridge JA.** 1991. Repression and induction of the nag regulon of *Escherichia coli* K-12: the roles of *nagC* and *nagA* in maintenance of the uninduced state. Mol Microbiol **5:**2053-2062.

75. **Postma PW, Lengeler JW.** 1985. Phosphoenolpyruvate:carbohydrate phosphotransferase system of bacteria. Microbiol Rev **49:**232-269.

76. **Saier MH, Jr., Reizer J.** 1992. Proposed uniform nomenclature for the proteins and protein domains of the bacterial phosphoenolpyruvate: sugar phosphotransferase system. J Bacteriol **174:**1433-1438.

77. **Saris PEJ, Palva ET.** 1987. The *ptsL*, *pel/ptsM* (*manXYZ*) locus consists of three genes involved in mannose uptake in *Escherichia coli* K12. FEMS Microbiol Lett **44:**371-376.

78. **Sun T, Altenbuchner J.** 2010. Characterization of a mannose utilization system in *Bacillus subtilis*. J Bacteriol **192:**2128-2139.

79. **Svitil AL, Chadhain S, Moore JA, Kirchman DL.** 1997. Chitin Degradation Proteins Produced by the Marine Bacterium *Vibrio harveyi* Growing on Different Forms of Chitin. Appl Environ Microbiol **63:**408-413.

80. **Barabote RD, Saier MH, Jr.** 2005. Comparative genomic analyses of the bacterial phosphotransferase system. Microbiol Mol Biol Rev **69:**608-634.

81. **Stonestrom A, Barabote RD, Gonzalez CF, Saier MH.** 2005. Bioinformatic analyses of bacterial HPr kinase/phosphorylase homologues. Res Microbiol **156:**443-451.

82. **Saier M, Hvorup R, Barabote R.** 2005. Evolution of the bacterial phosphotransferase system: from carriers and enzymes to group translocators. Portland Press, Portland, ME.

83. **Zúñiga M, Comas I, et al.** 2005. Horizontal gene transfer in the molecular evolution of mannose PTS transporters. Mol Biol and Evol **22:**1673-1685.

84. **Saier M, Roseman S.** 1976. Sugar transport. Inducer exclusion and regulation of the melibiose, maltose, glycerol, and lactose transport systems by the

phosphoenolpyruvate: sugar phosphotransferase system. J Biol Chem **251:**6606-6615.

85. **Campbell NA, Reece JB.** 2002. Campbell biology, 6th ed. Benjamin Cummings / Pearson, Boston, MA.

86. **Amin N, Peterkofsky A.** 1995. A dual mechanism for regulating cAMP levels in *Escherichia coli*. J Biol Chem **270:**11803-11805.

87. **Galinier A, Deutscher J.** 2017. Sophisticated Regulation of Transcriptional Factors by the Bacterial Phosphoenolpyruvate: Sugar Phosphotransferase System. J Mol Biol **429:**773-789.

88. **Bouma C.** 1991. Glucose transport in *Escherichia coli* and the marine bacterium *Vibrio furnissii*. Doctor of Philosphy, Johns Hopkins University, Baltimore, MD.

89. **Lux TM, Lee R, Love J.** 2011. Complete genome sequence of a free-living *Vibrio furnissii* sp. nov. strain (NCTC 11218). J Bacteriol **193:**1487-1488.

90. **Cochu A, Vadeboncoeur C, Moineau S, Frenette M.** 2003. Genetic and biochemical characterization of the phosphoenolpyruvate:glucose/mannose phosphotransferase system of *Streptococcus thermophilus*. Appl Environ Microbiol **69:**5423-5432.

91. **Neidhardt FC, Curtiss R.** 1996. *Escherichia coli* and *Salmonella*: cellular and molecular biology. ASM Press, Washington, D.C.

92. **Plumbridge J.** 1998. Control of the expression of the *manXYZ* operon in *Escherichia col*i: Mlc is a negative regulator of the mannose PTS. Mol Microbiol **27:**369-380.

93. **Plumbridge J, Kolb A.** 1993. DNA loop formation between Nag repressor molecules bound to its two operator sites is necessary for repression of the *nag* regulon of *Escherichia coli in vivo*. Mol Microbiol **10:**973-981.

94. **Plumbridge J.** 1995. Co-ordinated regulation of amino sugar biosynthesis and degradation: the NagC repressor acts as both an activator and a repressor for the transcription of the *glmUS* operon and requires two separated NagC binding sites. EMBO J **14:**3958-3965.

95. **Plumbridge J.** 1999. Expression of the phosphotransferase system both mediates and is mediated by Mlc regulation in *Escherichia coli*. Mol Microbiol **33:**260-273.

96. **Tanaka Y, Kimata K, Aiba H.** 2000. A novel regulatory role of glucose transporter *of Escherichia coli*: membrane sequestration of a global repressor Mlc. EMBO J **19:**5344-5352.

97. **Lee SJ, Boos W, Bouche JP, Plumbridge J.** 2000. Signal transduction between a membrane-bound transporter, PtsG, and a soluble transcription factor, Mlc, of *Escherichia coli*. EMBO J **19:**5353-5361.

98. **Plumbridge JA.** 1990. Induction of the *nag* regulon of *Escherichia coli* by *N*-acetylglucosamine and glucosamine: role of the cyclic AMP-catabolite activator protein complex in expression of the regulon. J Bacteriol **172:**2728-2735.

99. **Brosius J.** 1984. Plasmid vectors for the selection of promoters. Gene **27:**151-160.

100. **Horton RM, Cai ZL, Ho SN, Pease LR.** 1990. Gene splicing by overlap extension: tailor-made genes using the polymerase chain reaction. Biotech **8:**528-535.

101. **Horton RM.** 1995. PCR-mediated recombination and mutagenesis. SOEing together tailor-made genes. Mol Biotechnol **3:**93-99.

102. **Information NCBI.** pKK232-8 cloning vector, complete sequence, *on* National Center for Biotechnology Information. https://www.ncbi.nlm.nih.gov/nuccore/595745?report=fasta. Accessed December 10th, 2016.

103. **Tech B.** Sequence and plasmid map of pKK232-8, *on* Biovisualtech.com. http://www.biovisualtech.com/bvplasmid/pKK232-8_seq.htm. Accessed December 10th, 2016.

104. **Rodriguez RL, Denhardt DT.** 1988. Vectors : a survey of molecular cloning vectors and their uses. Butterworth Publishers, Stoneham, MA.

105. **International B.** 2009. NetPrimer, *on* Biosoft International. http://www.premierbiosoft.com/netprimer/. Accessed December 10th, 2016.

106. **Vaseeharan B, Ramasamy P, Murugan T, Chen JC.** 2005. *In vitro* susceptibility of antibiotics against *Vibrio spp.* and *Aeromonas spp.* isolated from *Penaeus monodon* hatcheries and ponds. Int J Antimicrob Agents **26:**285-291.

107. **Bustin SA, Benes V, et al.** 2009. The MIQE guidelines: minimum information for publication of quantitative real-time PCR experiments. Clin Chem **55:**611-622.

108. **Fu X, Liang W, Du P, Yan M, Kan B.** 2014. Transcript changes in *Vibrio cholerae* in response to salt stress. Gut Pathog **6:**47.

109. **Ye J, Coulouris G, Zaretskaya I, Cutcutache I, Rozen S, Madden TL.** 2012. Primer-BLAST: a tool to design target-specific primers for polymerase chain reaction. BMC Bioinformatics **13:**134.

110. **Studer S.** 2012. Defined Minimal Medium for *Vibrio fischeri*. http://www.glowingsquid.org/protocols_nr.php. Accessed May 7th, 2017.

111. **Maier T, Guell M, Serrano L.** 2009. Correlation of mRNA and protein in complex biological samples. FEBS Lett **583:**3966-3973.

112. **Maier T, Schmidt A, et al.** 2011. Quantification of mRNA and protein and integration with protein turnover in a bacterium. Mol Syst Biol **7:**511.

113. **Gygi SP, Rochon Y, Franza BR, Aebersold R.** 1999. Correlation between protein and mRNA abundance in yeast. Mol Cell Biol **19:**1720-1730.

114. **Trauger SA, Kalisak E, et al.** 2008. Correlating the transcriptome, proteome, and metabolome in the environmental adaptation of a hyperthermophile. J Proteome Res **7:**1027-1035.

115. **Gerlach RG, Holzer SU, Jackel D, Hensel M.** 2007. Rapid engineering of bacterial reporter gene fusions by using Red recombination. Appl Environ Microbiol **73:**4234-4242.

116. **Yamamoto S, Izumiya H, Morita M, Arakawa E, Watanabe H.** 2009. Application of lambda Red recombination system to *Vibrio cholerae* genetics: simple methods for inactivation and modification of chromosomal genes. Gene **438:**57-64.

117. **Datsenko KA, Wanner BL.** 2000. One-step inactivation of chromosomal genes in *Escherichia co*li K-12 using PCR products. Proc Natl Acad Sci USA **97:**6640-6645.

118. **Lesic B, Rahme LG.** 2008. Use of the lambda Red recombinase system to rapidly generate mutants in *Pseudomonas aeruginosa*. BMC Mol Biol **9:**20.

119. **Baltimore D.** 1970. RNA-dependent DNA polymerase in virions of RNA tumour viruses. Nature **226:**1209-1211.

120. **Mizutani S, Temin HM.** An RNA-dependent DNA polymerase in virions of *Rous sarcoma* virus, p 847-849. *In* (ed), Cold Spring Harbor Laboratory Press,

121. **Verma IM, Temple GF, Fan H, Baltimore D.** 1972. In vitro synthesis of DNA complementary to rabbit reticulocyte 10S RNA. Nature **235:**163-167.

122. **Rappolee DA, Mark D, Banda MJ, Werb Z.** 1988. Wound macrophages express TGF-alpha and other growth factors in vivo: analysis by mRNA phenotyping. Science **241:**708-712.

123. **Singer-Sam J, Robinson MO, Bellve AR, Simon MI, Riggs AD.** 1990. Measurement by quantitative PCR of changes in HPRT, PGK-1, PGK-2, APRT, MTase, and Zfy gene transcripts during mouse spermatogenesis. Nucleic Acids Res **18:**1255-1259.

124. **Robinson MO, Simon MI.** 1991. Determining transcript number using the polymerase chain reaction: Pgk-2, mP2, and PGK-2 transgene mRNA levels during spermatogenesis. Nucleic Acids Res **19:**1557-1562.

125. **Murphy LD, Herzog CE, Rudick JB, Fojo AT, Bates SE.** 1990. Use of the polymerase chain reaction in the quantitation of mdr-1 gene expression. Biochem **29:**10351-10356.

126. **Owczarek CM, Enriquez-Harris P, Proudfoot NJ.** 1992. The primary transcription unit of the human alpha 2 globin gene defined by quantitative RT/PCR. Nucleic Acids Res **20:**851-858.

127. **Tan SS, Weis JH.** 1992. Development of a sensitive reverse transcriptase PCR assay, RT-RPCR, utilizing rapid cycle times. PCR Methods Appl **2:**137-143.

128. **Liang P, Pardee AB.** 1992. Differential display of eukaryotic messenger RNA by means of the polymerase chain reaction. Science **257:**967-971.

129. **McPherson MJ, Møller SG.** 2000. PCR, 1st ed. BIOS Scientific Publishers, Oxford, England.

130. **Vandesompele J, De Preter K, et al.** 2002. Accurate normalization of real-time quantitative RT-PCR data by geometric averaging of multiple internal control genes. Genome Biol **3:**Research0034.

131. **Dheda K, Huggett JF, et al.** 2005. The implications of using an inappropriate reference gene for real-time reverse transcription PCR data normalization. Anal Biochem **344:**141-143.

132. **Bustin SA.** 2002. Quantification of mRNA using real-time reverse transcription PCR (RT-PCR): trends and problems. J Mol Endocrinol **29:**23-39.

133. **Bohlenius H, Eriksson S, Parcy F, Nilsson O.** 2007. Retraction. Science **316:**367.

134. **Bustin SA.** 2000. Absolute quantification of mRNA using real-time reverse transcription polymerase chain reaction assays. J Mol Endocrinol **25:**169-193.

135. **Bustin SA.** 2008. Molecular medicine, gene-expression profiling and molecular diagnostics: putting the cart before the horse. Biomark Med **2:**201-207.

136. **Bustin SA, Nolan T.** 2004. Pitfalls of quantitative real-time reverse-transcription polymerase chain reaction. J Biomol Tech **15:**155-166.

137. **Nolan T, Hands RE, Bustin SA.** 2006. Quantification of mRNA using real-time RT-PCR. Nat Protoc **1:**1559-1582.

138. **Bustin SA, Benes V, Nolan T, Pfaffl MW.** 2005. Quantitative real-time RT-PCR--a perspective. J Mol Endocrinol **34:**597-601.

139. **Bustin SA.** 2010. Why the need for qPCR publication guidelines?--The case for MIQE. Methods **50:**217-226.

140. **Bustin SA, et al.** 2013. The need for transparency and good practices in the qPCR literature. Nat Methods **10:**1063-1067.

141. **Fleige S, Pfaffl MW.** 2006. RNA integrity and the effect on the real-time qRT-PCR performance. Mol Aspects Med **27:**126-139.

142. **Jahn CE, Charkowski AO, Willis DK.** 2008. Evaluation of isolation methods and RNA integrity for bacterial RNA quantitation. J Microbiol Methods **75:**318-324.

143. **Becker C, Hammerle-Fickinger A, Riedmaier I, Pfaffl MW.** 2010. mRNA and microRNA quality control for RT-qPCR analysis. Methods **50:**237-243.

144. **Gutierrez L, Mauriat M, et al.** 2008. The lack of a systematic validation of reference genes: a serious pitfall undervalued in reverse transcription-polymerase chain reaction (RT-PCR) analysis in plants. Plant Biotechnol J **6:**609-618.

145. **Colton DM, Stoudenmire JL, Stabb EV.** 2015. Growth on glucose decreases cAMP-CRP activity while paradoxically increasing intracellular cAMP in the light-organ symbiont *Vibrio fischeri*. Mol Microbiol **97:**1114-1127.

146. **Camacho G.** Sugar transport by *Vibrio furnissii* by the phosphoenolpyruvate: sugar phosphotransferase system. Molecular cloning and sequencing of the *crr* gene encoding IIA^{Glc}. West Texas A&M University, Canyon, Texas.